SAND2023-01875R

FY23 Update: Surface Sampling Activities for the Canister Deposition Field Demonstration

Spent Fuel and Waste Disposition

Prepared for
US Department of Energy
Spent Fuel and Waste Science and Technology

A.W. Knight, D.G. Fascitelli, C.R. Bryan, S.G. Durbin, S. Verma, M. Maguire, and B. Nation
Sandia National Laboratories, Albuquerque, NM

April 14, 2023
Milestone No. M3SF-23SN010208033
SAND2023-XXXX R

Sandia National Laboratories
U.S. DEPARTMENT OF ENERGY NNSA

Sandia National Laboratories is a multimission laboratory managed and operated by National Technology & Engineering Solutions of Sandia, LLC, a wholly owned subsidiary of Honeywell International Inc., for the U.S. Department of Energy's National Nuclear Security Administration under contract DE-NA0003525.

DISCLAIMER

This information was prepared as an account of work sponsored by an agency of the U.S. Government. Neither the U.S. Government nor any agency thereof, nor any of their employees, makes any warranty, expressed or implied, or assumes any legal liability or responsibility for the accuracy, completeness, or usefulness, of any information, apparatus, product, or process disclosed, or represents that its use would not infringe privately owned rights. References herein to any specific commercial product, process, or service by trade name, trade mark, manufacturer, or otherwise, does not necessarily constitute or imply its endorsement, recommendation, or favoring by the U.S. Government or any agency thereof. The views and opinions of authors expressed herein do not necessarily state or reflect those of the U.S. Government or any agency thereof.

Prepared by
Sandia National Laboratories
Albuquerque, New Mexico 87185 and Livermore, California 94550

Sandia National Laboratories is a multimission laboratory managed and operated by National Technology & Engineering Solutions of Sandia, LLC, a wholly owned subsidiary of Honeywell International, Inc., for the U.S. Department of Energy's National Nuclear Security Administration under contract DE-NA0003525.

ABSTRACT

This report describes the results of a field demonstration of the proposed surface sampling techniques and plan for the multi-year Canister Deposition Field Demonstration (CDFD). The CDFD will evaluate salt deposition rates on three commercial 32PTH2 NUHOMS welded stainless steel storage canisters in Advanced Horizontal Storage Modules. Exposure testing is planned for up to 10 years and will incorporate periodic surface sampling campaigns. The goal of the planned dust sampling and analysis is to determine important environmental parameters that impact the potential occurrence of stress corrosion cracking on spent nuclear fuel (SNF) dry storage canisters. Specifically, measured dust deposition rates and deposited particle sizes will improve parameterization of dust deposition models employed to predict the potential occurrence and timing of stress corrosion cracks on the stainless steel SNF canisters. Previously, a preliminary sampling plan was developed, identifying possible sampling locations on the canister surfaces and sampling intervals; possible sampling methods were also described. Building from previous work, this report documents hand sampling from a spent nuclear fuel canister on a transfer skid mockup designed by Sandia National Laboratories. The sampling took place from a boom lift and salts were collected from mounted sample plates. The results of these efforts are presented in this report and compared to previous laboratory-controlled tests. The information obtained from the CDFD will be critical for ongoing efforts to develop a detailed understanding of the potential for stress corrosion cracking of SNF dry storage canisters.

This page is intentionally left blank.

ACKNOWLEDGEMENTS

This work was funded by the U.S. Department of Energy (DOE), Office of Nuclear Energy Spent Fuel and Waste Disposition Research and Development Program.

The authors would like to express their appreciation to Ned Larson of the DOE for his programmatic leadership and vision. We would like to thank Thad Vice and Adrian Perales for their efforts supporting this work. We greatly acknowledge the contributions and leadership of Sylvia Saltzstein, Geoff Freeze, and Scott Sanborn of Sandia National Laboratories to this project.

The authors would also like to thank Ramon Pulido for his technical review.

This page is intentionally left blank.

CONTENTS

This page is intentionally left blank.

LIST OF FIGURES

This page is intentionally left blank.

LIST OF TABLES

This page is intentionally left blank.

ACRONYMS

AHSM	Advanced Horizontal Storage Module
ASW	artificial sea water
CDFD	canister deposition field demonstration
DCSS	dry cask storage system
DI	deionized
DOE	US Department of Energy
DSC	dry shielded canister
FY	fiscal year
ISFSI	independent spent fuel storage installation
NE	Office of Nuclear Energy
NUHOMS	NUTECH Horizontal Modular Storage
PWR	pressurized water reactor
RH	relative humidity
SCC	stress corrosion crack
SFWD	Spent Fuel and Waste Disposition
SNF	spent nuclear fuel
SNL	Sandia National Laboratories
SOP	standard operating procedure
SS	stainless steel
TC	thermocouple

This page is intentionally left blank.

FY23 UPDATE: SURFACE SAMPLING ACTIVITIES FOR THE CANISTER DEPOSITION FIELD DEMONSTRATION

This report fulfills milestone M3SF-23SN010208033 in the Canister Deposition Field Demonstration (CDFD) work package (SF-23SN01020803). This work was sponsored under the Department of Energy's (DOE) Office of Nuclear Energy (NE) Spent Fuel and Waste Disposition (SFWD) campaign.

1 INTRODUCTION

Dry cask storage systems (DCSSs) for spent nuclear fuel (SNF) are designed to provide a confinement barrier that prevents the release of radioactive material, maintain SNF in an inert environment, provide radiation shielding, and maintain subcriticality conditions. SNF is initially stored in pools of water for cooling where the water also provides radiation shielding. As these pools get closer to capacity, dry storage systems are becoming the primary means of extended storage of SNF. After sufficient cooling in pools, SNF is loaded into a dry shielded canister (DSC) and placed inside a storage cask, where the canister is welded shut. The DCSS is then dried and decontaminated, and the system is moved to an on-site dry storage location for interim storage. An independent spent fuel storage installation (ISFSI) is designed for the interim storage of SNF, reactor-related greater than Class C waste, and other associated radioactive materials. Figure 1.1 and Figure 1.2 show the major components of typical horizontal and vertical dry storage cask systems for SNF.

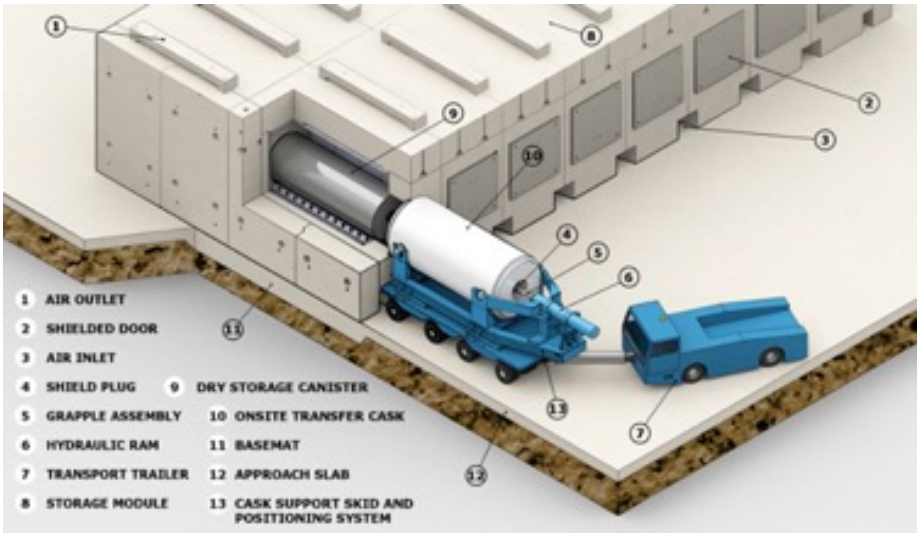

Source: https://www.orano.group/usa/en/our-portfolio-expertise/used-fuel-management/used-fuel-storage

Figure 1.1 Typical horizontal dry cask storage system.

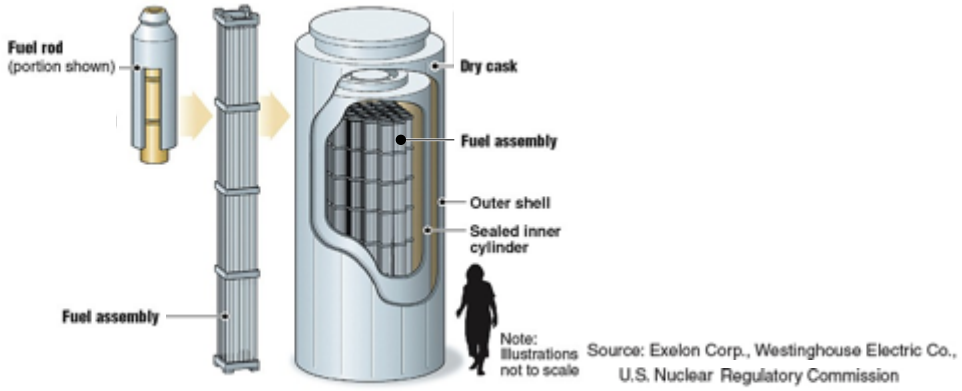

Figure 1.2 Typical vertical dry cask storage system.

Typically, the canisters are made of stainless steel (SS). The dry storage system is designed with an open volume between the canister and the storage cask or vault. Rejection of the decay heat is accomplished by air flowing from air inlets at the bottom to outlets at the top via natural convection. This passively cooled design also allows dust and salt from the environment into the system. These particulates may then collect on the surfaces of the canister. As the SNF cools, salts contained in the dust may deliquesce in the presence of moisture from the ambient relative humidity (RH) to form concentrated brines, which may contain corrosive species such as chlorides. These species can cause localized corrosion, called pitting. With sufficient stresses, these pits can evolve into stress corrosion cracks (SCCs), which could penetrate through the canister wall and allow communication from the interior of the canister to the external environment (Schindelholz *et al*., 2017).

1.1 Objective

Current surface sampling techniques for canisters loaded with SNF are unvalidated. One such technique employs robotic devices to collect deposition samples from the canister surface. The use of robotic surface sampling devices provides qualitative measurements of the salt and dust composition on the canister surface. However, the quantitative accuracy of these techniques has not been validated and therefore the efficiency is unknown. Current robotic sampling methods utilize vacuum suction approaches to collect dry samples and will not be effective for very high dust and salt deposition loads. These robotic devices disturb surface dusts, interfering with future sampling plans, as they traverse the canister and drag their tether across the surface. An example of a robotic sampling devices is shown in Figure 1.3.

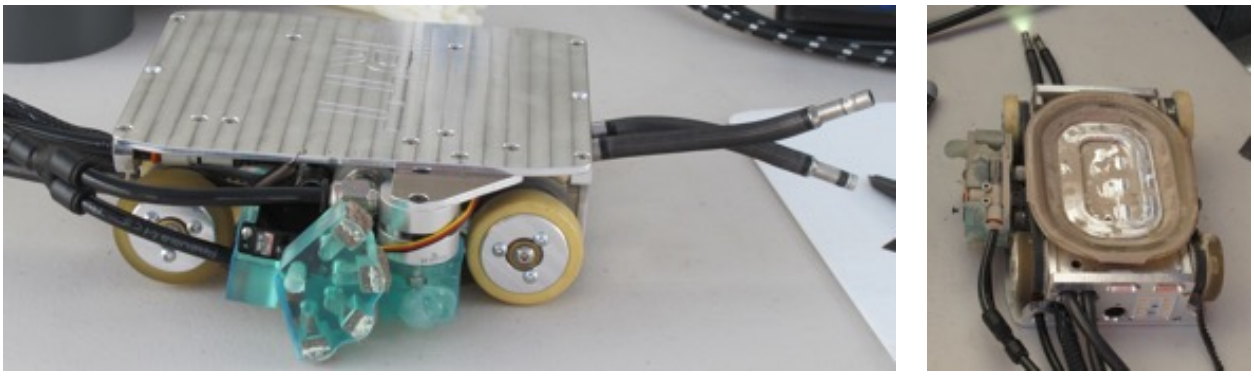

Figure 1.3 Robotic canister surface sampling device.

The objective of the CDFD is to measure the amount and composition of corrosive species (chloride salts) from marine coastal ambient air deposited onto prototypic SNF canisters, which can be used to validate the Pacific Northwest National Laboratory (PNNL) dust deposition model (Jensen *et al.*, 2021 and Suffield *et al.*, 2022). If performed properly, hand sampling of the canister surface will provide accurate information to be used for validation of robotic sampling methods and dust deposition modeling efforts. To facilitate surface sampling, the otherwise identical DCSSs will not contain SNF but rather electrical heaters to mimic the prototypic decay heat and thermal environment (Lindgren *et al.*, 2020). The DOE NE SFWD campaign has provided three Orano (formerly Transnuclear Inc.) NUTECH Horizontal Modular Storage (NUHOMS) 32PTH2 dry shielded canisters and Advanced Horizontal Storage Modules (AHSMs) for use in the study, illustrated in Figure 1.4. The 32PTH2 canister can hold thirty-two pressurized water reactor (PWR) fuel assemblies. Discussions are ongoing to locate a suitable facility to host this long-term deposition study. An ISFSI near a marine coastal environment would be ideal to provide a better understanding of a harsh, yet realistic, condition. This is because it is expected that the salts in these environments will likely contain chlorides.

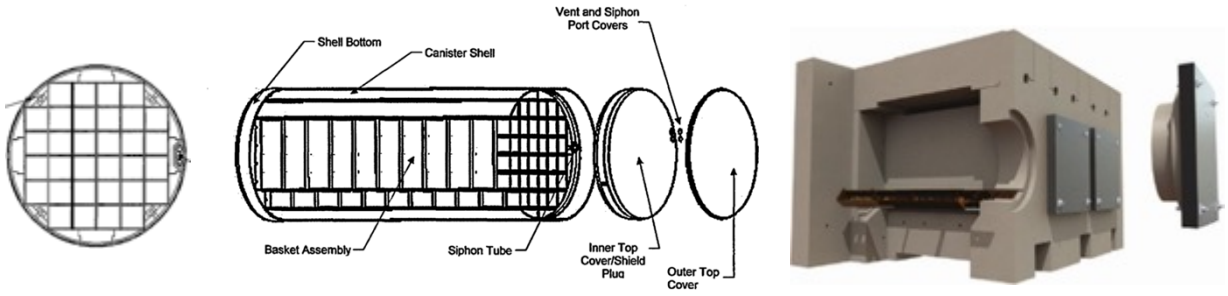

Figure 1.4 32PTH2 spent fuel canister (end view—left, side view—center) and Advanced Horizontal Storage Modules (sectioned side view—right).

The study will include three identical DCSSs. One system will represent a canister loaded with roughly the maximum allowed heat load, another will represent a canister loaded with one quarter of the maximum heat load, and the third canister will be used as an unheated control. The three canisters will be designed to simulate three decay heats.

1. 0 kW decay heat as a control case. Canister will be loaded with heater assemblies and insulation to perform as a backup if other DCSSs fail. The surface temperature of the control canister is expected to be equivalent to the surrounding ambient temperature and therefore the achievable RH can be high enough for salts to deliquesce (Schaller *et al.* 2022).
2. 10 kW decay heat to represent canisters that have been stored for several years and more susceptible to deliquescence than the higher-powered canister because of cooler surface temperatures. The maximum surface temperature is expected to reach ~90 ºC based upon preliminary testing and thermal modeling (Fascitelli *et al.,* 2022, Suffield *et al.*, 2022).
3. 40 kW decay heat to represent a freshly loaded system with short-cooled fuel. The maximum allowable heat load for a 32PTH2 is 37.2 kW (Transnuclear Inc., 2017). The decay heat will be decreased at various intervals to determine how concentration, composition, and location of deposits vary with decay heat and associated air flow velocities and patterns. The maximum surface temperature is expected to reach ~210 ºC based upon thermal modeling (Suffield *et al.*, 2022).

After some period of time to be determined based on a combination of modeling and ambient aerosol host site characterization, the canisters will be inspected for salt composition and concentration at various locations on the canister as described in Section 2.2. One series of simulated field testing of this surface sampling activity has been performed, with more planned for the future. The results of this test series are presented and discussed in Section 4. Establishing a standard operating procedure (SOP) that ensures highly defensible salt deposition data prior to canister deployment to a permanent host site is critical to project success. This report details the progress made on rehearsing, assessing, and refining hand sampling procedures and activities.

2 CANISTER SAMPLING PLAN

The current plan is to place a series of 2 × 2 sample grids on the surface of each test canister. The grids will be placed at 20 proposed locations as described in Section 2.2. During sampling activities, the canister will be extracted from the AHSM and onto the roller rails of a transfer skid so that the canister surface can be accessed by the sampling team. Continued simulated field testing and the determination of which equipment will be available for canister extraction from the AHSM will inform additional sampling locations of interest. A depiction of the position of the canister in relation to the AHSM during sampling is shown in Figure 2.1.

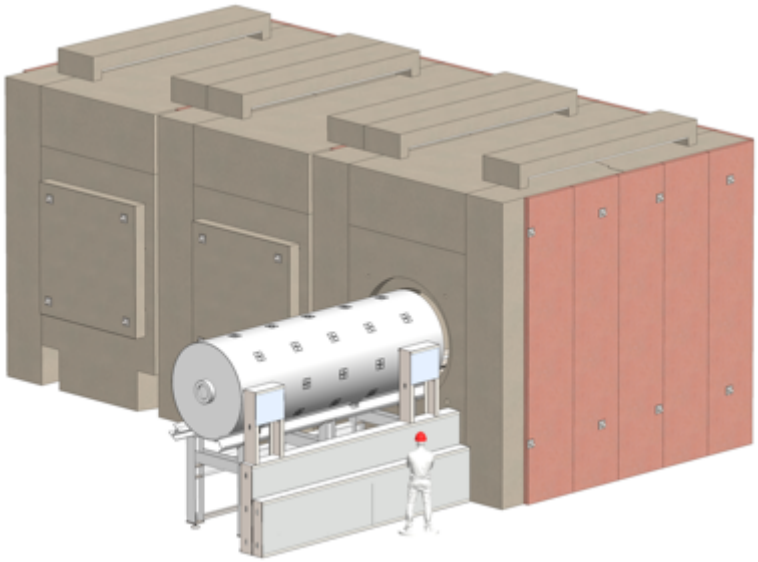

Figure 2.1 Computer model of canister on transfer skid mockup positioned in front of AHSM for hand sampling.

2.1 Sample Grids

Each canister will be instrumented with thermocouples (TCs) to monitor the external shell temperature. The exterior surface of the canister will be instrumented with type-T TCs to provide a minimum of one temperature measurement for each surface sample location. Type-T TCs were selected because they offer greater accuracy at the temperatures expected on the canister. As described in detail in Bryan *et al.* (2021), the area around each TC location on the exterior of the canister will be sampled on a periodic basis for surface deposits in a regular pattern as depicted in Figure 2.2. The central TC location is indicated by the purple circle in the center in Figure 2.2. Each of the four colored squares represents a sampling location approximately 7.5 × 7.5 cm (3.0 × 3.0 in.) and two types of samples will be collected at each location – a dry sample and a wet sample during every sampling event (see Bryan *et al.*, 2021 for details). This large surface area for sampling increases the likelihood that collected salt concentrations will be large enough to be accurately quantified, even when relatively low salt loads on the canister surface are present.

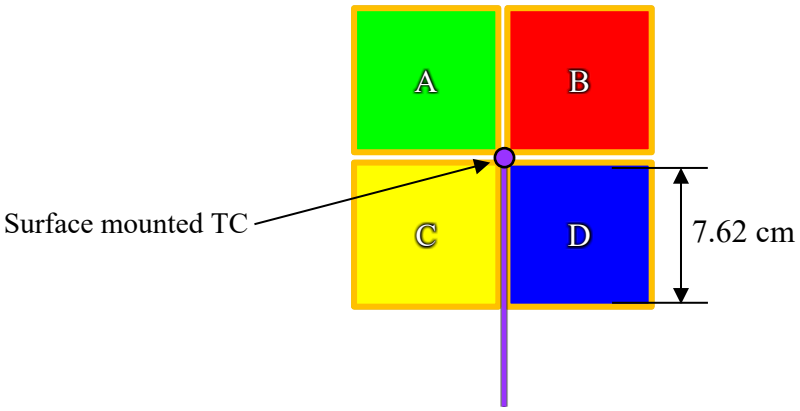

Figure 2.2 Surface deposition sampling pattern.

An important consideration is to make these temperature measurements in a manner that minimizes any flow disturbance of the naturally induced air flow over the canister surface carrying the particulates of interest. To minimize air flow disturbance on the surface of the canister, smaller type-T TCs with diameter of 0.81 mm (0.032 in.) will be used, and the sheaths will be routed just above the canister support rails as shown in Figure 2.3. The TCs will run straight longitudinally along the canister shell and then route circumferentially to the location of interest.

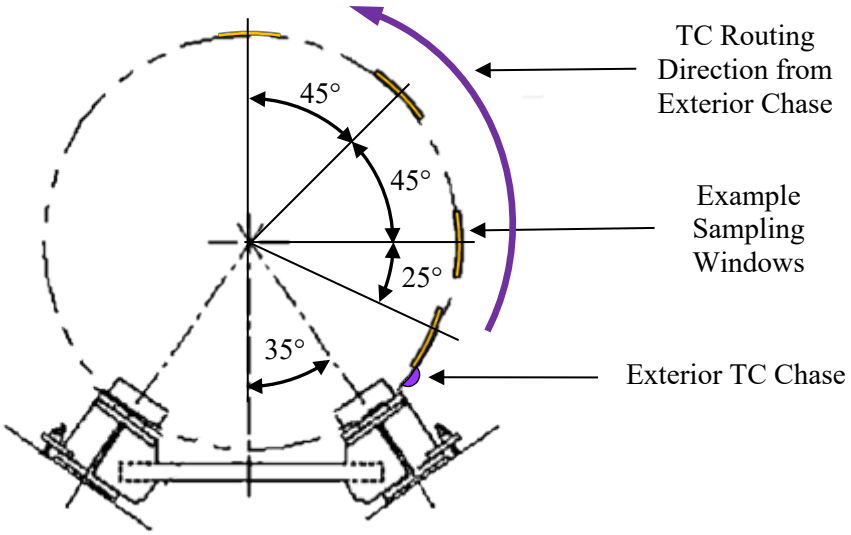

Figure 2.3 End view of the canister and support rails showing example sampling locations. Adapted from Figure B.3.1-7 [Transnuclear, 2016].

The TCs will be secured to the canister shell by spot-welding SS shim stock to the canister. An equally important consideration for the exterior TCs is to ensure that enhanced corrosion is not a consequence of their implementation. Previous investigations into the susceptibility of enhanced corrosion for this attachment method found that there were no signs of a large corrosion response due to the attached TC wires and shims (Knight *et al.*, 2022).

Previous evaluations of engine enamel and blackening agents as marking materials for the sampling grids on the canister determined that these materials may not be sufficiently robust to withstand the maximum expected canister surface temperature of ~200 °C for the entire duration of the CDFD test. Thus, TC wires and shims will likely serve an additional purpose as markings for orientation of the sampling template on the canister.

2.2 Canister Sampling Layout

Sampling locations have been chosen to cover a wide range of different parameters that are anticipated to affect salt and dust deposition on the canister surface. These parameters are described in detail in Bryan *et al.* (2021). Canister surface orientation (e.g., canister top, sloping upper surface, vertical sides, sloping lower surface) is one such parameter pertinent to the simulated field testing. The yellow boxes in Figure 2.3 indicate the circumferential sample locations of interest. A total of 20 sampling grids were proposed for evaluation during the simulated field testing, with five sampling grids along the axial length of the canister for each of the circumferential locations. The longitudinal locations correspond to just inside the innermost bottom weld, the canister center, a longitudinal location just inside the bottom of the inner lid at the top of the canister, and points halfway between these three longitudinal locations. The spacing between sampling grids along the length of the canister is approximately 0.91 m (36 in.). A rendering of the canister and the 20 initially proposed sampling locations is shown in Figure 2.4.

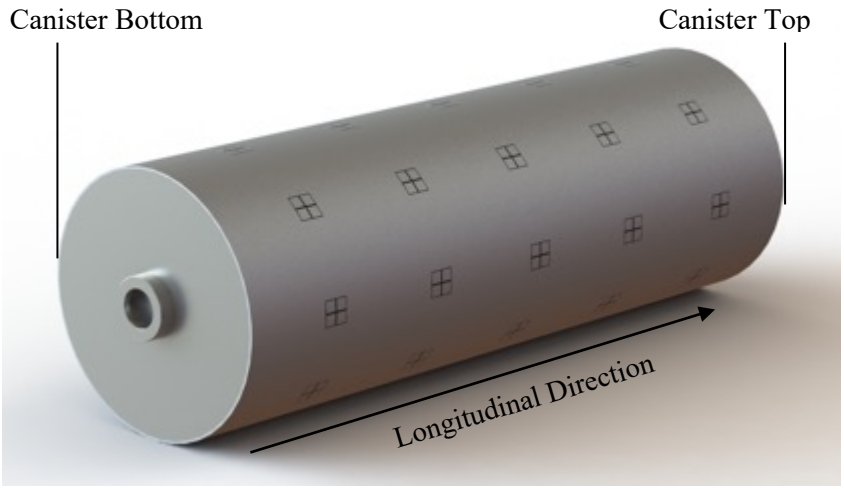

Figure 2.4 Rendering of dry shielded canister with proposed sampling layout.

2.3 Periodic Sampling Schedule

A possible sampling schedule for each location is summarized in Figure 2.5 (Bryan et al., 2021) and was constructed to maximize the ability to collect cumulative undisturbed salt deposition and deposition rates over smaller intervals. The four sibling locations around the TC should provide comparable results due to proximity. Specifically, at each sampling location on the canister, the first grid block (A) will be sampled during the first sampling campaign, one year into the test. During the second sampling campaign, grid block B will be sampled for the first time, and grid block A will be resampled. During each sampling campaign, a new grid block will be sampled, and some subset of the already sampled blocks will be resampled. Each newly sampled block provides cumulative dust and salt load information; resampled blocks provide yearly data (Bryan *et al.*, 2021).

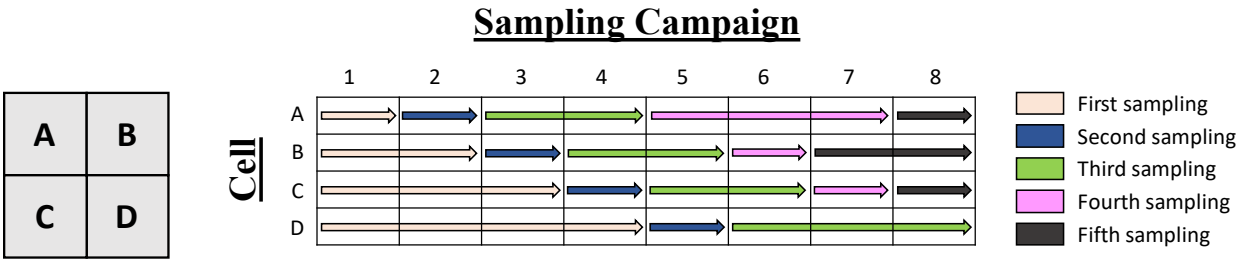

Figure 2.5 Sampling grid and possible sampling schedule (Bryan *et al.*, 2021).

2.4 Hand Sampling Template

To define and constrain the area that is being sampled on the canister surface, a hand sampling template will be pressed against the surface and the area within the template window will be sampled (Knight *et al.*, 2022). The template has been 3D printed and has sufficient flexibility to conform to the canister surface. A polymer gasket on the bottom of the template ensures a good seal to the canister surface as well. A rendering of the hand sampling template is shown in Figure 2.6.

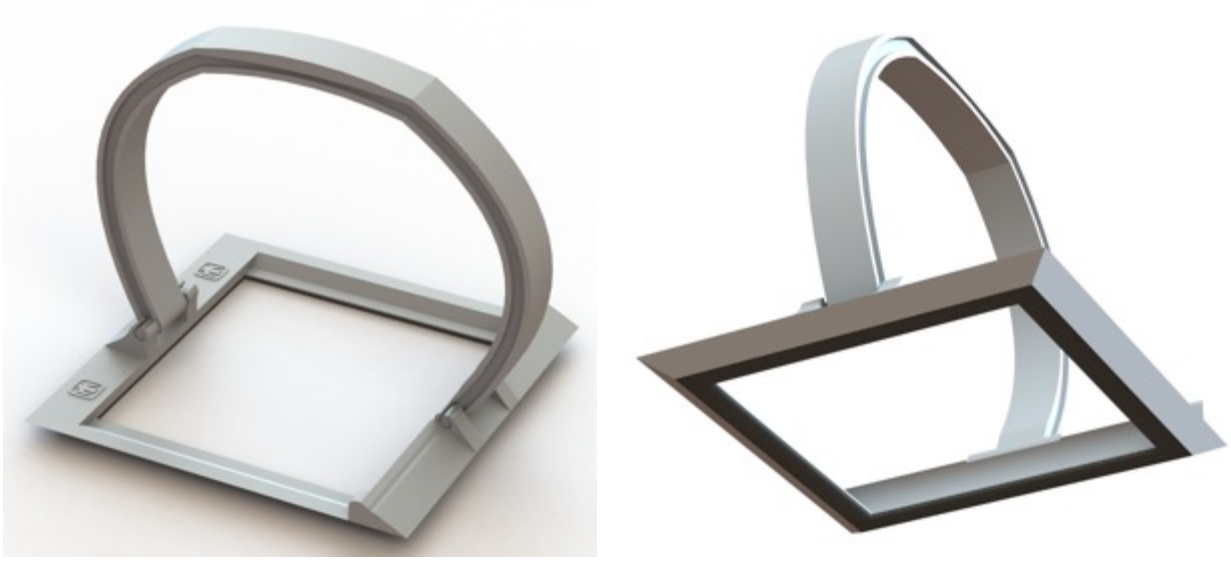

(a) (b)

Figure 2.6 (a) Top rear isometric and (b) bottom front isometric views of the 3D-printed hand sampling template.

3 SIMULATED FIELD TESTING OF HAND SAMPLING TECHNIQUES FOR THE CDFD PROJECT

In ISFSI dry storage canister dust sampling campaigns to date, remote methods (robots and long probes) have largely been used to sample canister surface deposits. However, little is known about the sampling efficiency of such methods—uncertainties exist in both the actual size of the area sampled and in the efficiency of dust and salt collected. Because of the unproven nature of these techniques, the decision was made to use hand sampling to collect and quantify dust and salts deposited on the canisters used in the CDFD project. Initial development of hand-sampling techniques was carried out in a laboratory setting, using plates cut from a Sandia National Laboratories (SNL) canister mockup built in 2016 to evaluate weld residual stresses (Enos and Bryan, 2016). The plates had a curvature similar to the CDFD canisters, and had a mill finish similar to (slightly rougher than) the CDFD canisters. The hand sampling technique involved a 3D-printed sampling template that was pressed against the metal surface to define a sampling region with dimensions of 7.6 × 7.6 cm (3 × 3 in.). Moist sponges were used to collect the salts from the metal surface. Two sponges were used to clean the defined region. With practice, average sampling efficiencies of ~90% were consistently achieved. The laboratory tests to develop the hand-sampling techniques has been documented in the following SFWST reports (Knight *et al.,* 2022, Schaller *et al.,* 2022)

Although the method was proven to be effective in a laboratory setting, it was important to test the hand sampling techniques under more realistic conditions. In the field, dust will be collected from vertical and overhanging canister surfaces while the canister is on a transfer skid immediately in front of the AHSM overpack. The central axis of the canister will be 2.7 m (8 ft.-10 in.) above ground level during sampling and will require an articulating boom lift to reach the canister surfaces. Limited space within the boom lift will impose constraints on hand sampling, as will requirements for stand-off distances to ensure the lift does not contact the canister. In addition, access to some parts of the canister will be limited by components of the transfer skid. Due to the complexity and physical limitations that would arise during sampling of the canisters, it was determined that a simulated field test was necessary. A transfer skid mockup was designed and fabricated in Tech Area III of Sandia National Laboratories to assist the sampling team in identifying and rehearsing a proper procedure for surface sampling (Fascitelli *et al.,* 2022). A prototypic spent fuel canister was placed on the mockup transfer skid, and tests were carried out to evaluate the hand sampling approach, modifying techniques and sample locations as necessary to accommodate the access limitations imposed by the boom lift and the transfer skid. This report documents the initial simulated field hand-sampling test.

Rendered engineering drawings of a loaded canister transfer skid and the transfer skid mockup are shown in Figure 3.1 and Figure 3.2. Once the heaters have been turned off, the canisters will be allowed to cool within their overpacks. The canisters will then be pulled from the overpacks with a hydraulic ram on the transfer skid. Once on the transfer skid, some parts of the canister will be obstructed or inaccessible. For safety, personnel will not be allowed to climb onto the skid; access to the surface will be accomplished using a boom lift or similar device. The width of the transfer skid, which is significantly wider than the canister, will restrict approach to the lower parts of the canister. Trunnion posts on the skid will also obscure some parts of the canister. The gap between the trunnion posts is about 0.3 m (11 in.). Finally, the canister will not be extracted completely from the overpack, and boom lift access will be restricted by the proximity to the overpack. The trunnion posts and the base of the transfer skid have been faithfully included in the transfer skid mockup (Figure 3.2).

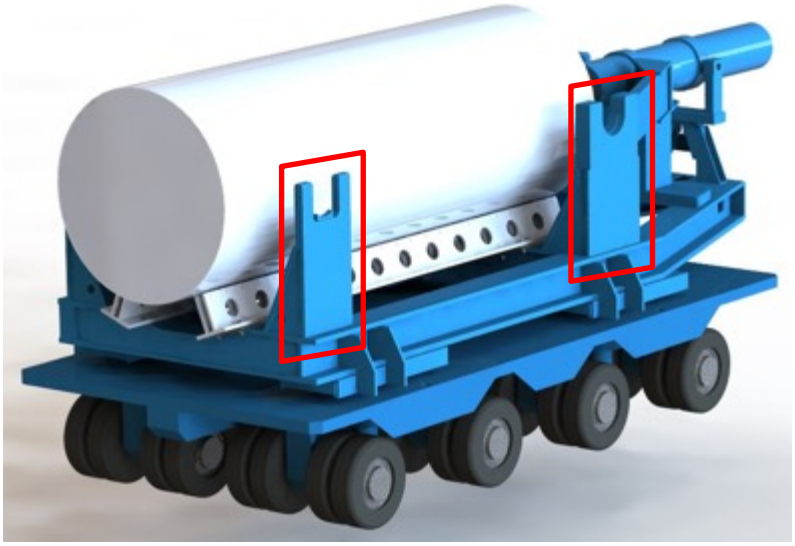

Figure 3.1 Rendering of transfer skid used for inserting and extracting canister into/from AHSM. Red boxes indicate the trunnion posts of the transfer skid, which will obstruct parts of the canister during sampling.

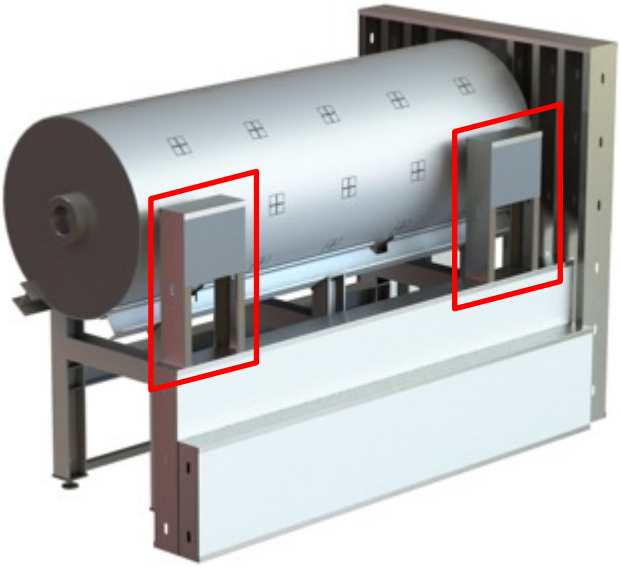

Figure 3.2 Rendering of transfer skid mockup used for sampling rehearsals. Red boxes indicate the representative trunnion posts.

The simulated field test took place in Tech Area III of Sandia National Laboratories in Albuquerque, New Mexico. A 32PTH2 canister on the as-built transfer skid mockup is shown in Figure 3.3. As part of the simulated field test, two activities were performed. The first activity was a dry run, in which the boom lift, with the analyst and the boom lift operator, moved to various positions around the canister to rehearse how the samples would be collected. No actual sampling was performed. This activity evaluated the accessibility of the proposed sampling locations and provided an opportunity to discuss and practice the sampling procedure. For the second activity, salt-coated sampling plates were mounted to the canister

surface and the salts were collected off the plates using a sampling template and sponges to evaluate the efficiency of the sampling method. Once the salt-coated plates were mounted to the canister surface, the sample collection was completed within 2 hours. There was little wind, and the sample plates were mounted to the leeward side of the canister (east side, prevailing winds came from the west), so it was not expected that the samples were significantly affected by dust and salt deposition after being mounted onto the canister.

Figure 3.3 Transfer skid mockup and canister at the Surtsey site located in Tech Area III of Sandia National Laboratories.

The mockup sampling exercise had three specific goals:

1. Practice and refine sampling techniques and procedures for the canister surface, given the limited access and constraints imposed by the boom lift,
2. Familiarize analysts with the equipment that will be used in the field,
3. Characterize the accuracy of the sampling methodology under more realistic conditions (e.g., sample orientation, access limitations) than were possible in the laboratory testing.

3.1 Sampling Plates

SNL routinely deposits a known salt load onto metal surfaces using a fogging chamber or, for more precise work, an inkjet printer. However, the dimensions of a dry storage canister preclude using these techniques to deposit salts directly onto the canister surface. Instead, small SS plates were coated with artificial sea water (ASW) and mounted onto the canister surface at the desired sampling locations. The plates are shown in Figure 3.4. Each plate was cut to approximately 23 × 23 cm (9 × 9 in.) and was rolled to match the outer diameter of the canister (0.89 m (35 in.) radius of curvature). After rolling the plates, 0.81 mm (0.032 in.) TC sheaths were attached to the surface using SS shims that were spot-welded to the surface of the plate. Thermocouples were located at the center of each 2 × 2 sampling grid (Figure 3.4a), and also at opposing corners. The sheaths ran up from the bottom of each plate to simulate their placement on the actual CDFD canisters. Additional shims were spot-welded onto the plate to serve as alignment features for the sampling template and define the 7.62 cm (3 in.) squares within each sampling grid for alignment of the sampling template (Figure 3.4b).

(a)

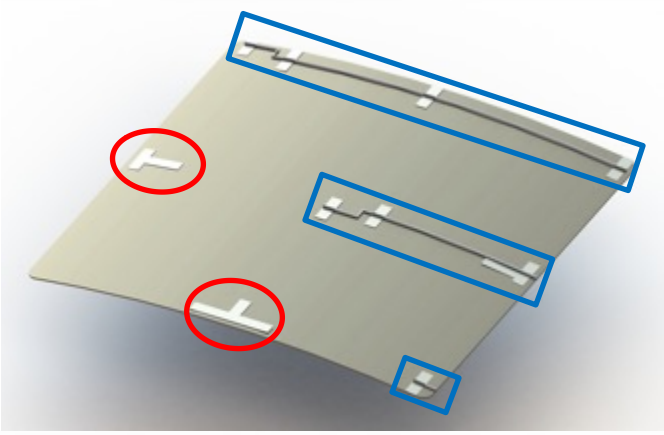

(b)

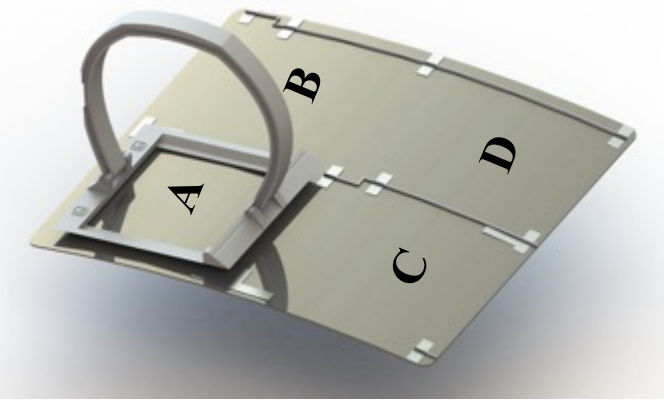

Figure 3.4 Renderings of (a) a sampling plate instrumented with TC wires (blue boxes) and alignment shims (red circles); (b) a sampling plate with a hand sampling tool aligned to sampling region A.

After the thermocouples and shims had been added to each plate, a 2.5 cm (1 in.) Parafilm® square was applied to the approximate center of each sampling square within the 2 × 2 grid. A inkjet printer was then used to coat the plates with ASW to achieve a final salt load of ~ 100 µg/cm^2. This procedure has been previously described (Schindelholz and Kelly, 2010). After coating, the plates were stored in plastic bins with desiccant cartridges until immediately prior to the sampling test. At that time, the Parafilm® witness coupons were carefully removed and transferred to labeled sample vials; they were later measured to

determine the actual salt loads in each of the four squares on each plate. The plates were then mounted onto the canister surface using double-sided foam tape for the test.

3.2 Evaluation of Canister Accessibility

The first activity performed on January 26th, 2023 evaluated the accessibility of the proposed sampling locations with the canister on the transfer skid mockup. The purpose of this activity was to determine if the sampling locations could be hand sampled by personnel on the boom lift, given the access limitations represented by the transfer skid and the wall of the overpack and to practice canister sampling at prototypic height. The sampling locations are described in a previous report and presented in Figure 2.4 (Bryan *et al.*, 2021; Knight *et al.*, 2022). A picture of the canister on the transfer skid mockup from the side being sampled is shown in Figure 3.5. Potential obstructions to sampling include the base of the skid itself, which limits proximity to the lower parts of the canister; the trunnion posts, simulated on the mockup; and the front face of the AHSM overpack, which limits the ability of the boom lift to approach the top end of the canister. It is worth noting that the AHSM front wall in the mockup is approximately the width of the transfer skid, but in the field, it will extend several feet beyond the width of the transfer skid. The transfer skid is approximately 3 m (10 ft.) wide, and the entire width of the row of three AHSMs is about 12.9 m (42 ft.).

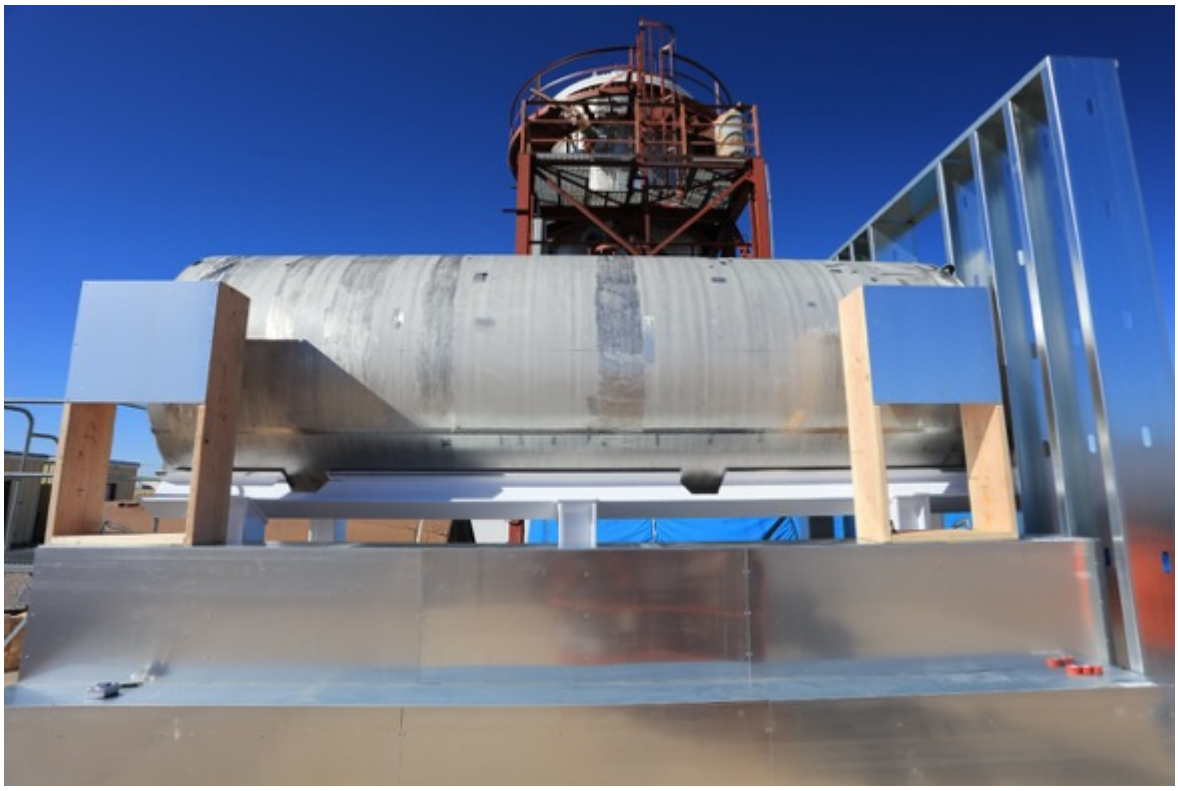

Figure 3.5 Photograph of the canister on the transfer skid mockup.

In the first activity of the simulated field testing, the salt-coated plates were not applied to the canister surface, and no sampling was carried out. The sampling team, consisting of the analyst and the boom lift operator, rehearsed the sampling motions to determine if the proposed sampling areas could be accessed. The boom lift operator not only operated the lift but also aided in the sampling by passing materials to the analyst. In this dry run, the analyst had a dry sponge and the hand sampling template. At each location, the boom lift operator would position the lift basket to allow for the analyst to reach the surface, if possible. The analyst would place the hand sampling template against the surface and practice the

sampling motions with a dry sponge. The analyst would then pass the sponge to the boom lift operator to be placed in a labeled sample tube. This exercise was performed with two different analysts, analyst 1 and analyst 2, with the same boom lift operator.

For each analyst, the same sample locations were evaluated. These are shown on a flattened canister map in Figure 3.6. The locations form a grid from U to Z across the longitudinal length of the canister and 1 to 4 from the top of the canister to a location just above the transfer skid rail (positions below the transfer skid rail are not accessible for sampling). Positions U through Y reflect the original sampling plan (Figure 2.4) and are equally spaced across the length of the canister. With the canister fully extracted from the overpack, it became apparent that positions U3 and U4, and positions Y3 and Y4, cannot be accessed because of the trunnion posts. The physical position of the trunnion posts can be seen in Figure 3.7. One possible mitigation strategy for sample grids U3 and U4 is to partially extract the canister and to sample the grids when they are in a position corresponding to a column that the trunnion posts do not interfere with (column W, for example). For sampling grids Y3 and Y4, this positioning cannot be done, so as an alternative, it was proposed to collect samples from a new sampling row, Z, between the trunnion post and the AHSM wall.

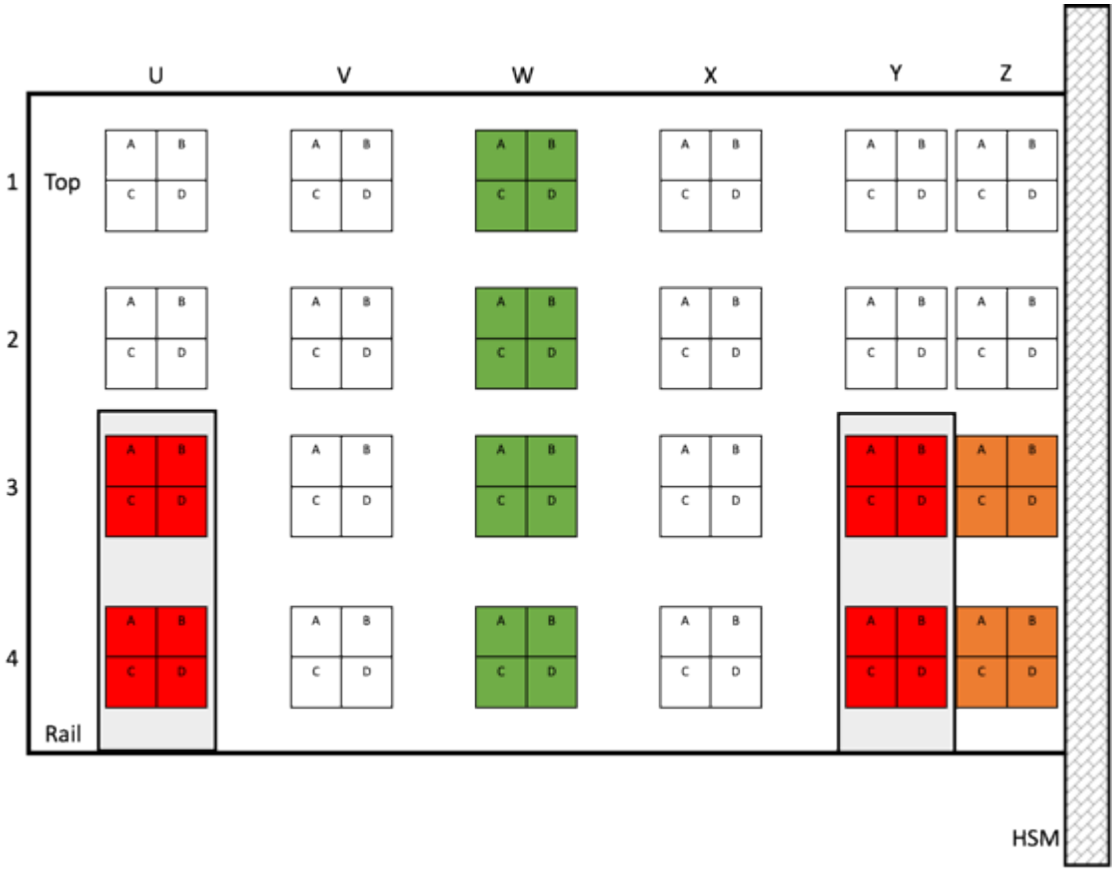

Figure 3.6 Sampling rehearsal locations to evaluate positioning. W1-W4 (green) were easily accessible for both analysts. W1-W4 were assumed to represent U1-U2, V1-V4, X1-X4, Y1-Y2, and Z1-Z2 (white), so these grids were not explicitly evaluated. The locations behind the trunnion posts, U3-U4 and Y3-Y4, were inaccessible (red). The locations Z3-Z4 (orange) were only accessible by one analyst and challenging for the boom lift to get arranged. *This image is not to scale.

Figure 3.7 The canister on the transfer skid and the location of the trunnion posts.

Each analyst, working with the boom lift operator, practiced sampling at positions W1-W4 and Z3-Z4. Positions W1-W4 reflect the accessibility of the majority of the proposed canister sampling sites (U1-U2, V1-V4, X1-X4, and Y1-Y2), while locations Z3-Z4 are particularly challenging because of the narrow 40 cm (16 in.) gap between the trunnion post and the AHSM front wall. Sample grid locations Z3 and Z4 were accessible from the boom lift for only one of the analysts.

Locations W1-W4 were accessible to both analysts, although the boom lift operator had to maneuver carefully to clear the base of the sampling skid. Figure 3.8 shows an analyst placing the sampling template against the surface at position W4. Row 4 was determined to be the most difficult position among the four locations tested from column W for both analysts. It is clear in the picture that the lowest position on the canister is a long reach from the boom lift, requiring that the analyst lean far out. However, with the necessary safety constraints, the position was accessible to both analysts. Both the analyst and boom lift operator were equipped with a harness and self-retracting lanyard for fall protection. Figure 3.9 shows an analyst rehearsing the sampling method at position W1 on the top of the canister. It is clear in this figure that the boom lift carriage can only accommodate the lift operator and one analyst at a time. It also became clear during the practice run that the boom lift operator will have to assist with the sampling. A plan was developed in which the analyst would place the sampling template against the canister surface, and the lift operator would hand them a sponge; the analyst would then run the sponge across the sample area and pass it back to the lift operator to place in a sample container. This would be repeated with a second sponge to maximize salt recovery. Note that during the access test, dry sponges were used, and sample collection was only simulated.

Figure 3.8 Positioning the boom lift to sample position W4 near the bottom of the canister. In this picture, the analyst is placing the sampling template against the canister surface.

Figure 3.9 Sampling position W1 near the top of the canister. In this picture, the analyst is passing a sponge to the boom lift operator to place in a sample tube.

Positions W1-W4 were accessible for the analysts and presented no insurmountable limitations or obstructions that would prevent successful sampling. The lowermost position, W4, was somewhat awkward to reach because the lift position required that the analyst squat and reach between the rails of

the lift carriage to collect the sample. To sample W3, the boom lift did not need to move. The analyst simply stood up and the sampling region was easily accessible. Position W2 was also easy to sample after positioning the lift close enough for the analyst to comfortably reach the canister surface. Position W1, on the top of the canister, required moving the boom lift directly over the canister and having the analyst work in a prone position, reaching through the rails of the lift carriage. Given the limited space within the lift, this was an awkward position for both the boom lift operator and the analyst; however, once the boom lift was in place, the surface was relatively easy to reach.

Unlike positions W3-W4, sampling at Z3-Z4 was less successful. The first challenge was the positioning of the boom lift. Figure 3.10 shows the boom lift in a position that allowed the analyst to reach between the trunnion post and the AHSM front wall. However, this positioning of the boom lift is unrealistic and would not be possible during actual field sampling due to the existence of the AHSM front walls. It was possible for the lift to wedge into the corner formed by the transfer skid and the AHSM wall and for the analyst to reach into the gap, but this was logistically difficult given the limited space within the lift. The space between the trunnion post and the AHSM is approximately 40 cm (16 in.). Because of the trunnion post, the lift could not approach the canister as closely as it had done for the W samples. Only the taller of the two analysts was able to reach the canister surface in row Z. For these reasons, it was decided that column Z would be omitted as a possible sampling position. Also, given that there was no mitigation for the two lowermost samples in column Y, sample locations Y3 and Y4 would be omitted from the study as well.

Figure 3.10 An analyst and the boom lift operator positioning itself in an impossible location to increase the accessibility of Z3.

3.2.1 Revised Sampling Locations Due to Limited Accessibility

Following the dry run, revised sampling procedures and locations were proposed. Changes were required because locations behind the trunnion posts and in-between the trunnion post and the AHSM front wall proved to be impossible to sample. The revised sampling positions are shown in Figure 3.11. The proposed procedure for sampling column U is to extract the canister partially from the overpack and sample when column U aligns positionally to another sampling column that affords greater accessibility (column V or W, for example). When the canister is partially extracted, U1-U4 will be sampled, as the trunnion post would not be in the way. Then, the canister will be fully extracted to sample the V, W, and X columns, as well as grids Y1 and Y2. There is no feasible way to sample Y3 and Y4. Therefore, in the revised sampling plan, samples at position Y3 and Y4 and the entire Z column, proposed as an alternative to the Y samples, will be omitted.

Importantly, it is not currently known if it will be feasible to partially extract the canister from the AHSM. If this is not possible, then samples U3 and U4 will also have to excluded, as the trunnion posts would also interfere with sampling of those locations.

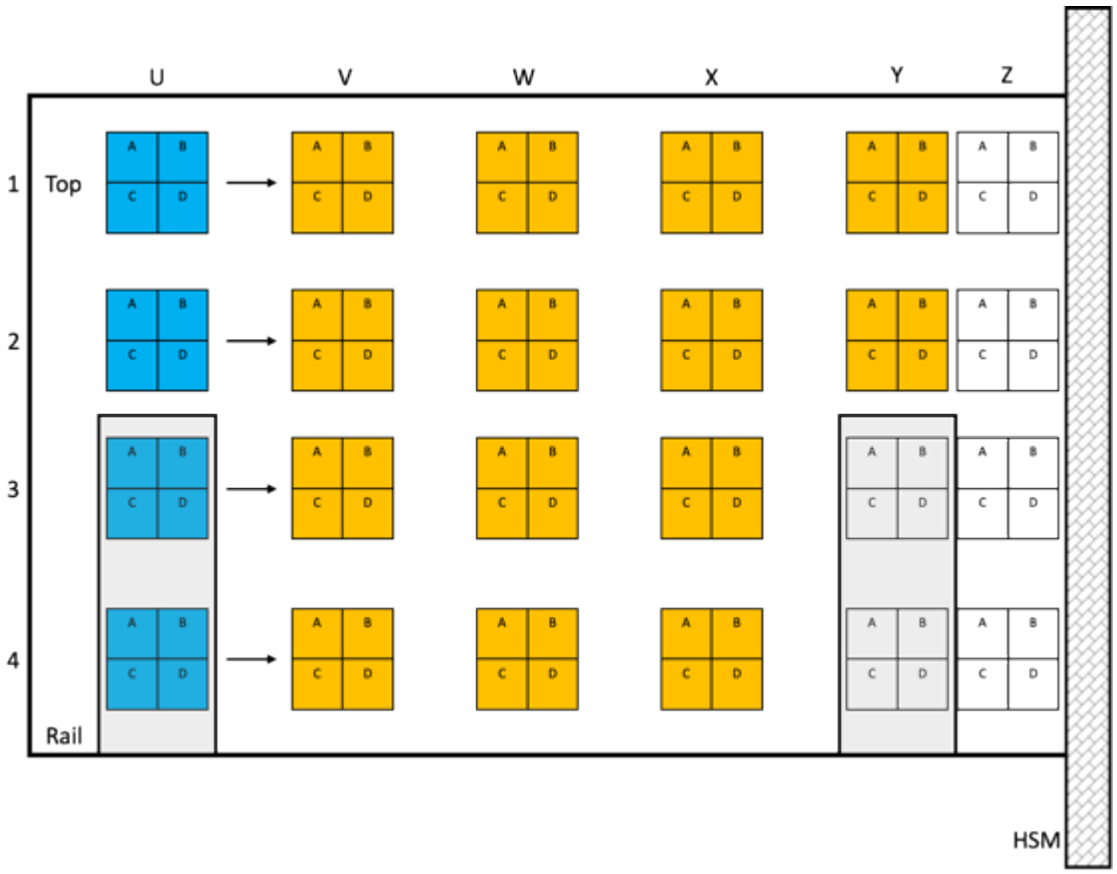

Figure 3.11 Revised sampling locations informed by accessibility evaluations. For this sampling procedure, the canister will be extracted so that locations U1- U4 (blue) are in the V position. Once U1-U4 are sampled, the canister will be completely pulled out of the ASHM to sample V1-V4, W1-W4, X1-X4, and Y1-Y2 (yellow). Position Z1-Z4 and Y3-Y4 were omitted (white). *This image is not to scale.

3.3 Canister Sampling

The second exercise involved sampling the salts off the sampling plates (Section 3.1) that were mounted to the canister in positions W1-W4 (Figure 3.12). The longitudinal column W was selected because the accessibility was high, and it therefore provided a good first opportunity to evaluate how sampling the canister surface compared to previous laboratory tests on mockup plates (Knight et al., 2022). After removing the Parafilm® witness coupons (Section 3.1) from the middle of the four test squares on each plate (Figure 3.13), the entire plate was mounted to the canister using double-sided tape (Figure 3.14).

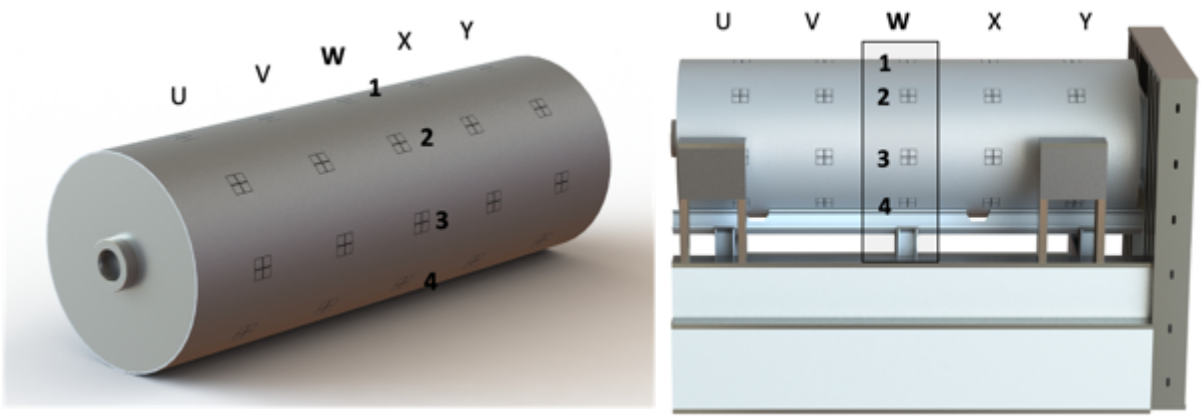

Figure 3.12 Locations where the sample plates were mounted to the canister for the hand sampling test.

Figure 3.13 Pictures of the four sample plates after the Parafilm® were removed, prior to mounting on the canister.

Figure 3.14 Sampling plate placement on canister surface at position W3 with plate already positioned at W4.

3.3.1 Sampling Procedure

Once the plates were mounted on the canister, salt deposits from each of the 4 sample areas within each sample plate were collected. Four samples were collected from each of the four sampling plates, for a total of 16 samples. The plates were identified as 1 through 4, corresponding to each circumferential location in the W column of the sampling layout (Figure 3.12). Within each sample plate, the 4 sampling quadrants were identified as A, B, C, and D (Figure 3.15). Each analyst sampled half of each of the four plates. Analyst 1 first sampled the left side of each plate (1A, 1C, 2A, 2C, 3A, 3C, 4A, and 4C) then was replaced on the lift by analyst 2, who sampled the right side of each plate (1B, 1D, 2B, 2D, 3B, 3D, and 4B, and 4D). The boom lift operator positioned the lift basket and assisted the analysts for the collection of each sample. The samples were collected from bottom to top to minimize the potential to contaminate the lower sampling locations with material falling off the lift.

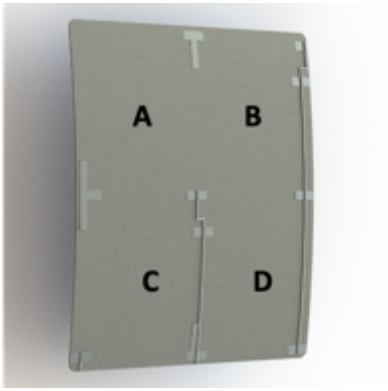

Figure 3.15 Sample plate showing the sampling quadrants: A, B, C, and D.

During the sampling activity, the boom lift operator would position the lift basket close enough to the canister surface to allow for the analyst to reach the surface comfortably (Figure 3.16). The boom lift basket contained deionized (DI) water, Kimwipes, tweezers, gloves, storage jars, several sampling templates, and 16 labeled and pre-tared sample tubes, each containing two 2.5 cm (1 in.) cubes of blue Tru-CLEAN® polyurethane sponge. For each sample, the analyst would extract the sponges from the sample tube with the tweezers and place them in a storage jar with DI water. After saturating the sponges, the analyst gently squeezed the sponge to eject most of the water, leaving the sponge damp (consistent with laboratory tests (Knight *et al.*, 2022)), and placed them in a second storage jar handled by the lift operator. The analyst would then get into position and place the sampling template against the plate surface. The placement of the hand sampling tool is described in Section 3.1, using the TC wires and shims to aid in tool alignment. The lift operator, using the tweezers, would pass one moist sponge to the analyst, and the analyst would use the sponge to sample the area defined by the sampling template. The template alignment and surface sampling can be seen in Figure 3.17 and Figure 3.18 for samples 4C and 3D, respectively. The analyst passes the sponge back to the lift operator, and the lift operator, using the tweezers, places the sponge into the sample tube. Figure 3.19 shows the analyst passing a sponge to the boom lift operator after sampling quadrant 1A on top of the canister. Figure 3.20 shows the surface of 4D being sampled with a moist sponge. At each location, after using the first moist sponge, a second sponge was applied to collect any remaining salts.

Figure 3.16 Boom lift approach to allow for Analysts to access the canister surface.

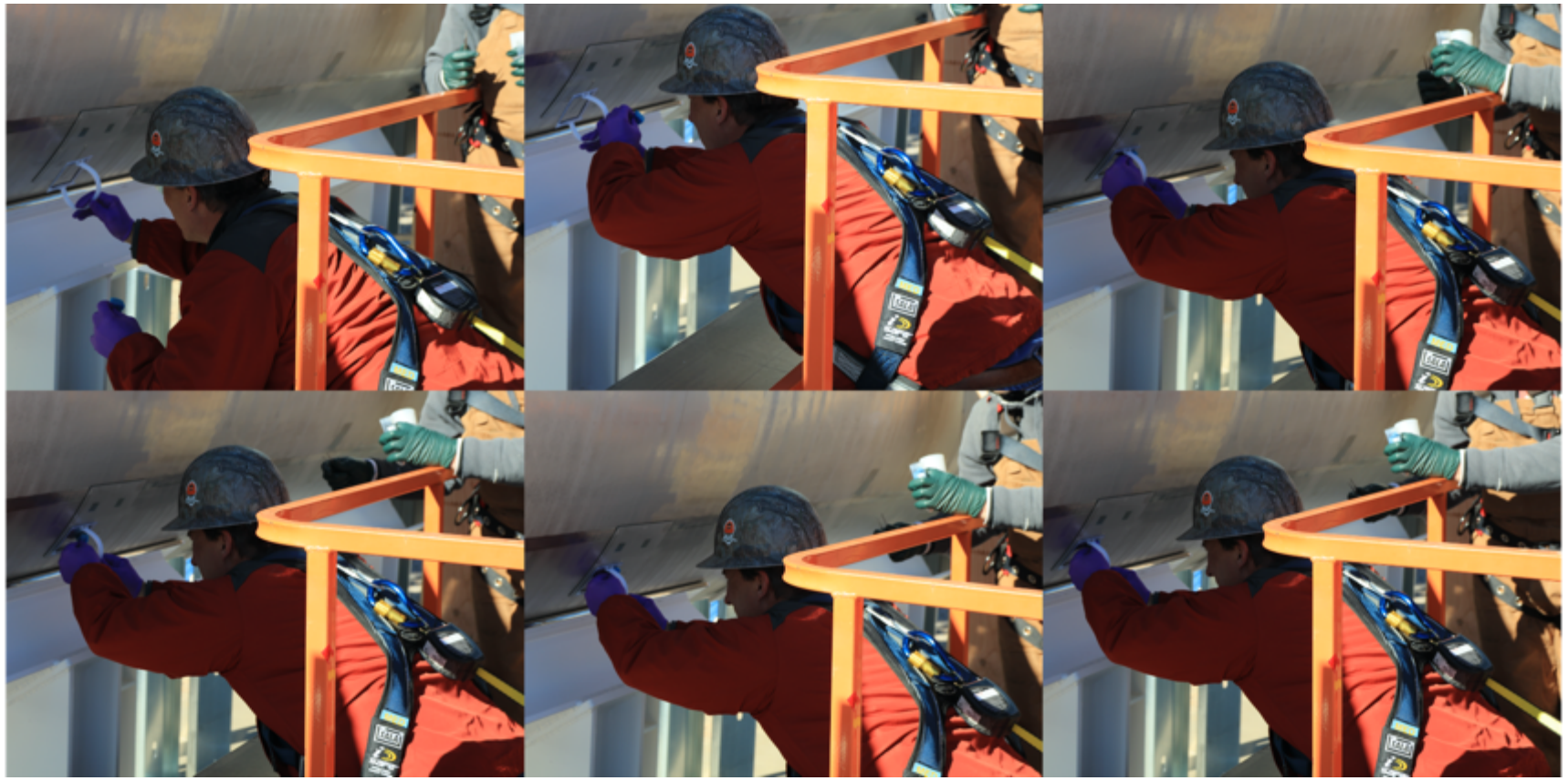

Figure 3.17 A picture showing the analyst aligning the sampling template and collecting the surface deposits, while sampling 4C.

Figure 3.18 A picture showing the analyst aligning the sampling template, taking the sponge from the boom lift operator, sampling the surface, and passing the sponge back to the boom lift operator, while sampling 3D.

Figure 3.19 A picture showing the analyst passing a sponge to the boom lift operator after sampling location 1A.

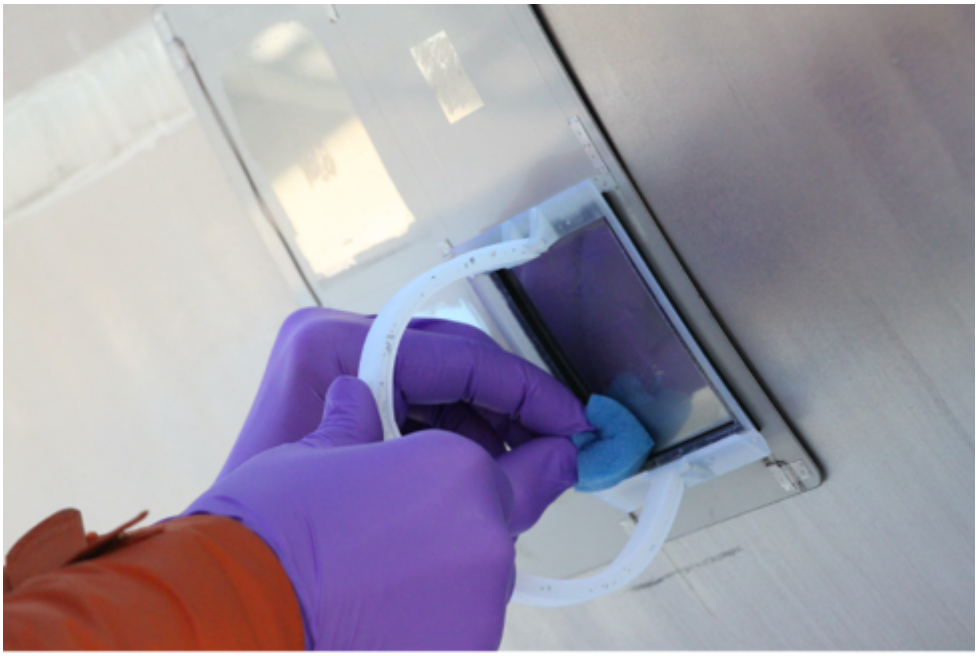

Figure 3.20 A picture showing the analyst using the moist sponge to sample the surface in location 4D. Samples 4A and 4C have already been sampled.

At each location, the analyst would sample individual quadrants. After sampling one quadrant, the analyst would then repeat the procedure to sample the vertically adjacent quadrant at the same location. This required pulling back into the boom lift and preparing a second set of moist sponges and a second pre-tared sample vial. A picture of the analyst preparing the sponges for a second quadrant on plate 1 is shown in Figure 3.21. A picture of the fully sampled plate 3 is shown in Figure 3.22 for plate 3. Effort was made to prevent cross contamination – gloves were changed frequently, and DI water was used to rinse the tweezers, the sampling template, and other materials as needed. The procedure was consistent from analyst to analyst to minimize sampling bias due to procedural differences.

After the plates had been fully sampled, they were removed from the canister and the collected samples were transferred to the laboratory for analysis.

Figure 3.21 A picture showing the analyst prepare the second set of sponges to sample 1C after sampling 1A.

Figure 3.22 A picture showing sample plate 3 after all quadrants were sampled. It is clear from this picture that some water and possibly salt was left behind on 3B.

This page is intentionally left blank.

4 RESULTS OF SIMULATED FIELD TESTING

Following completion of the surface sampling, the salts were leached from the sponge samples and the Parafilm® witness coupons. The conductivity of the leachates was then measured to evaluate the sampling efficiency. The method to measure conductivity is described in Knight *et al.* (2022). Briefly, the sample sponges and Parafilm® witness coupons were leached with DI water by adding 40 mL and 10 mL, respectively, to each sample vial. The sponges were repeatedly raised, compressed, and released with a steel spatula to equilibrate the fluid in the sponges with the bulk solution, as this was determined to be critical to effectively leach the salts from the sponges (Knight *et al.*, 2022). After leaching for several minutes, the conductivities of each of the witness coupon and sponge samples were measured using a Jenway 4510 conductivity meter and a Jenway conductivity probe. Measured conductivities were normalized by the sampled area, 1 in^2 (6.5 cm^2) for the witness coupons and 8 in^2 (51.6 cm^2) for the sample cells, yielding units of $\mu S/cm^2$. The area of each sample was 8 in^2, because the area of the 1 in^2 Parafilm® witness coupon had to be subtracted from the overall area defined by the sampling template (9 in^2). Sampling efficiencies were calculated by comparing the surface-area-normalized measured conductivities for each square in the sample grid, in $\mu S/cm^2$, to the measured conductivity of the corresponding Parafilm® coupon. The measured conductivities for each Parafilm® witness coupon and for the corresponding sponge samples are shown in Figure 4.1. It is assumed that the surface-area-normalized conductivity of the Parafilm® witness coupon is representative of the conductivity of the entire sample square. However, it should be noted that the conductivities of the 4 witness coupons on each individual sample plate vary with a standard deviation of 1-5% depending on the plate (Table 4.1). This could indicate that deposition across the plate was not entirely uniform or could simply be due to experimental error—for instance, when cutting the Parafilm® witness coupons, an error of 0.5 mm in one dimension of a witness coupon corresponds to a 2% error in the reported conductivity. It should also be noted that when salt deposition was accomplished using a fogging chamber, and measurements were monitored using many witness coupons on each plate, the deposited salt variability was ~25% across the surface (Knight *et al.*, 2022). Using the salt printer resulted in a much more uniform salt load across the metal surface.

Table 4.1 Average conductivity and standard deviation for the witness coupons on each sample plate.

Plate	Average Conductivity of 4 Witness Coupons ($\mu S/cm^2$)	Standard Deviation (%)
1	257.3	2.09
2	250.5	3.85
3	269.8	1.11
4	259.7	5.53

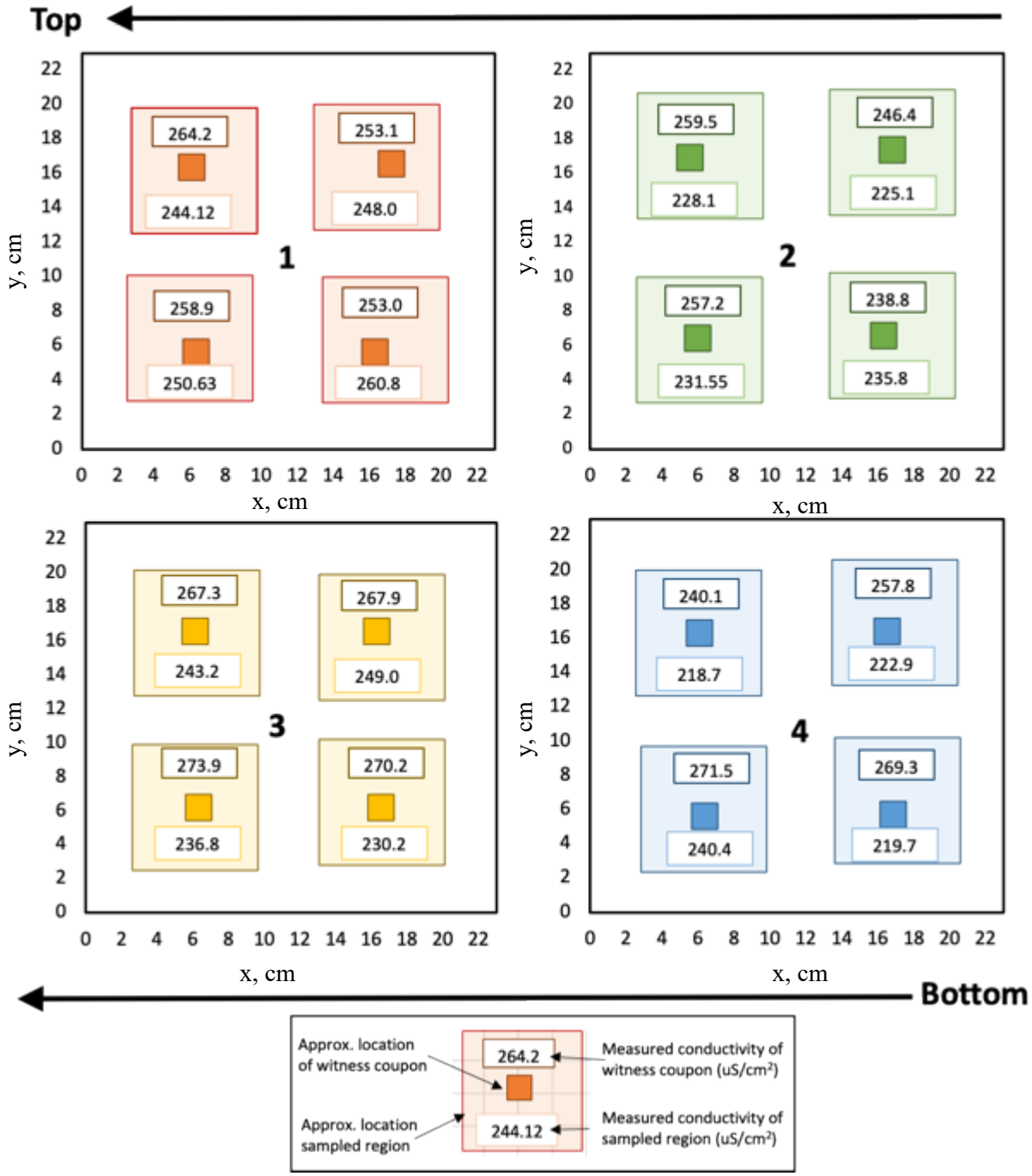

Figure 4.1 The measured conductivity in µS/cm² of the witness parafilm pieces (top number with darker outline) and sponge samples (bottom number with lighter outline). Note that sample locations are approximate.

4.1.1 Hand Sampling Tool Positioning

In addition to the measured conductivities of each sample, the sample position was nominally measured as well to evaluate the placement of the hand sampling tool. This is important because during the CDFD project, the canisters will be pulled from the overpack on a periodic basis, and the sampling locations will be sampled multiple times over the course of the project. Therefore, it is important to sample the same exact location, as best as possible, every time that particular quadrant is sampled. The witness coupon and sampled positions were estimated by measuring the location of the center of each feature. The witness coupons left an obvious imprint on the SS surface (however, the margins were not always clear), and the sampled regions were visually shinier than the unsampled regions. Figure 4.1 shows the approximate positions of the witness coupon and the sampled areas.

Figure 4.2 shows the approximate position of each of the witness coupons and sampling positions for all 4 sampling plates. It is clear from this plot that there was some variability in the position of the Parafilm® witness coupons within each sample square and that the position was only approximately the mid-point of the sample quadrant on the sample plate. However, due the relatively low variability in overall salt load across the sample plates, it is unlikely that the location of the witness coupons has any significant impact on the estimation of the conductivity of the sampled area.

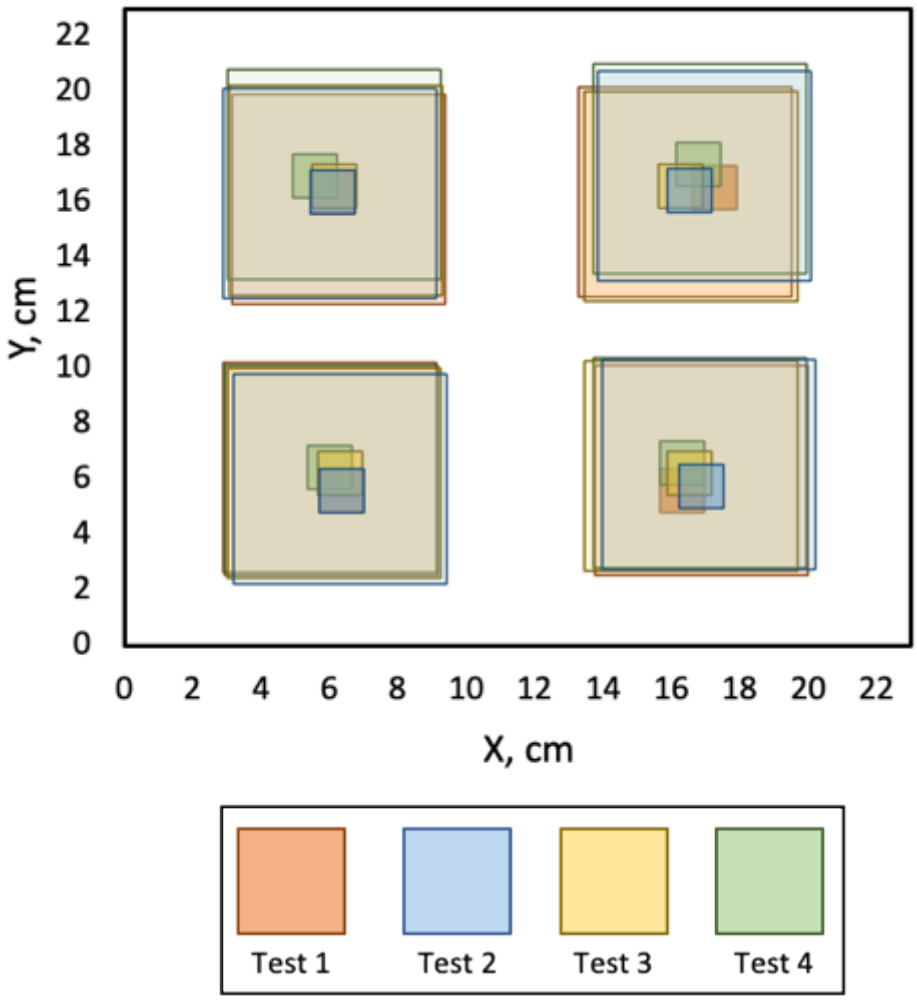

Figure 4.2 Plot showing the approximate location of each of the sampled areas and the witness Parafilm® pieces to demonstrate location variability from plate to plate.

The placement of the sampling template varied somewhat from plate to plate but was relatively consistent overall. During placement, the template was aligned with the shims and TC wires, as described in Section 3.1. The most significant misalignment occurred on quadrants A and B for plates 2 and 4. For quadrant A, the sample from plate 2 was placed higher up on the plate than the rest of the samples; for quadrant B, the placement on plates 2 and 4 was high and to the right. Two possible reasons for these deviations in alignment are the lack of an upper shim for alignment and/or the sampling angle of these two plates (Figure 4.3). For all samples, the analyst aligns with the inside edge of the outer shims and the midline of the middle shim attached to the center TC . All quadrants had 3-4 shims for alignment, which is generally enough. However, because the viewing angles were not always straight on, the spots where the 4th alignment shim was missing may have made alignment more difficult. Quadrants C and D had 4 shims on all plates, and the alignment of these two quadrants were the most consistent. For plate 2, it is possible that for quadrants A and B, the sampler was aligned vertically with the inside edge of the central TC shim, as the approach angle to place the sampling template made the top line hard to see or align with. For plate 4 at bottom of the canister, the upper right corner does not have shim to align with, and due to the awkward approach angle, it may have been challenging to spot the other alignment shims, causing a slight misalignment of the sampling template.

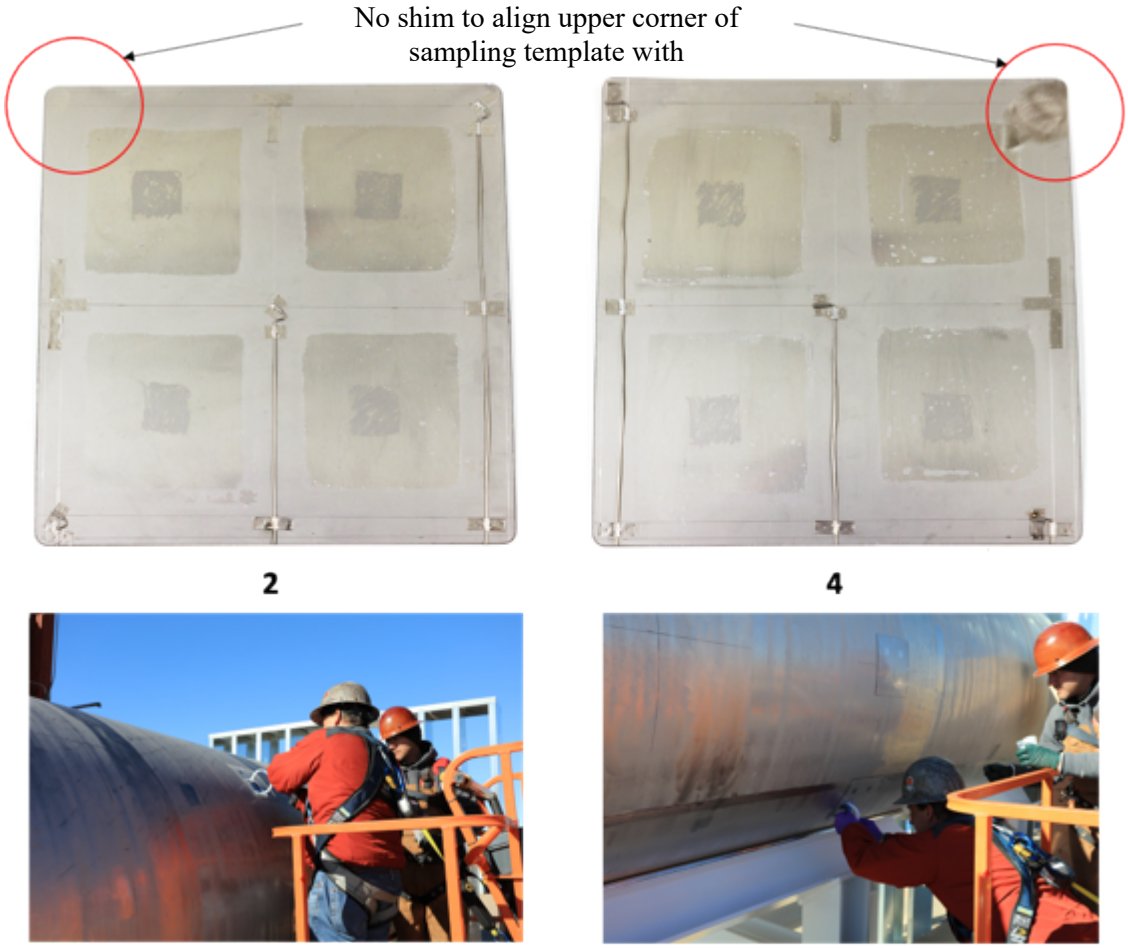

Figure 4.3 Picture of plates 2 and 4 showing quadrants with 3 shims and how the shim quantity along with the sampling angle may have challenged the alignment of the hand sampling tool.

4.1.2 Sampling Efficiency

The results of the sampling efficiency for each quadrant are shown in Figure 4.4. The percent salt recovered was calculated using Equation 1:

$$\%Salt\ Recovered = \frac{Conductivity_{\ sponges}}{Conductivity_{parafilm}} * 100 \qquad \text{(Equation 1)}$$

where the conductivity is the measured surface-area-normalized conductivity in μS/cm^2. The % salt recovery ranges from 81.6% to 103.1%, with an overall average of 91 ± 5 %. There was no significant dependence upon the identity of the analyst. Analyst 1 averaged 90 ± 3 % salt recovery and analyst 2 averaged 92 ± 7% salt recovery. Some of the under-sampling could be attributed to the actual surface area samples being slightly smaller than the surface within the sample window defined by the template. The actual area sampled in each quadrant sampled was estimated by measuring the area of the cleaned region, which could be readily identified visually (Figure 3.22). Bluebeam Revu 20 was used to trace and calculate the area of this sampled region, and the measured values were compared to the ideal surface area of 8 in^2. For example, sample 4B (top right on plate 4 in Figure 4.3), had a recovery of 86.5%, which was lower than average, and some spots within the sample window were not sampled. Specifically, it was observed during sampling that the top middle section, along the edge of the sample window, was frequently missed, because of interference from the handle of the sampling template. Once identified, extra effort was made to minimize the impact of this obstruction. While incomplete sampling impacted the overall recovery, it is not the only cause of the under-sampling. Figure 4.6 shows a plot of the % salt recovery versus the % area sampled. If incomplete coverage of the sample area was the only source contributing to incomplete recovery, the samples would fall on the unity line shown on the plot. Most of the samples fall below the line, which suggests there is another source that is causing less than 100% recovery. Another source that contributed to incomplete recovery was leaving excess water/brine behind on the surface after sampling. Evidence of this can be seen in Figure 3.22, where water droplets and dried salt are evident in the sampling window after sampling occurred. This was more evident after the samples dried and specks of white salt were visible on the metal surface within the sample window (Figure 4.3).

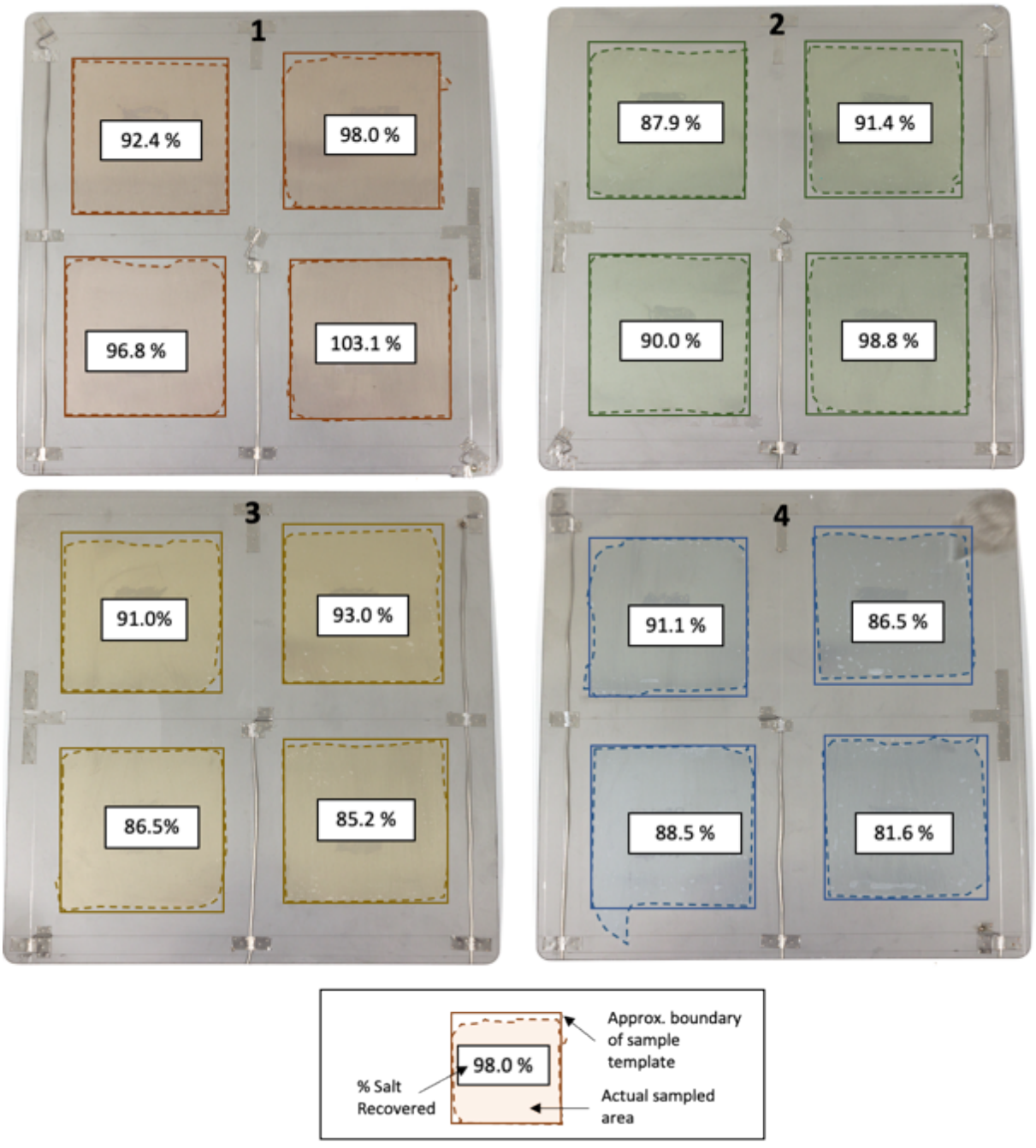

Figure 4.4 Sampling efficiency for each quadrant from sample plates 1-4. The sampling efficiency is the % of the value determined from the witness Parafilm® piece. The solid lines represent the size of the sample window (3 in^2) and the dashed line traces the actual sampled region.

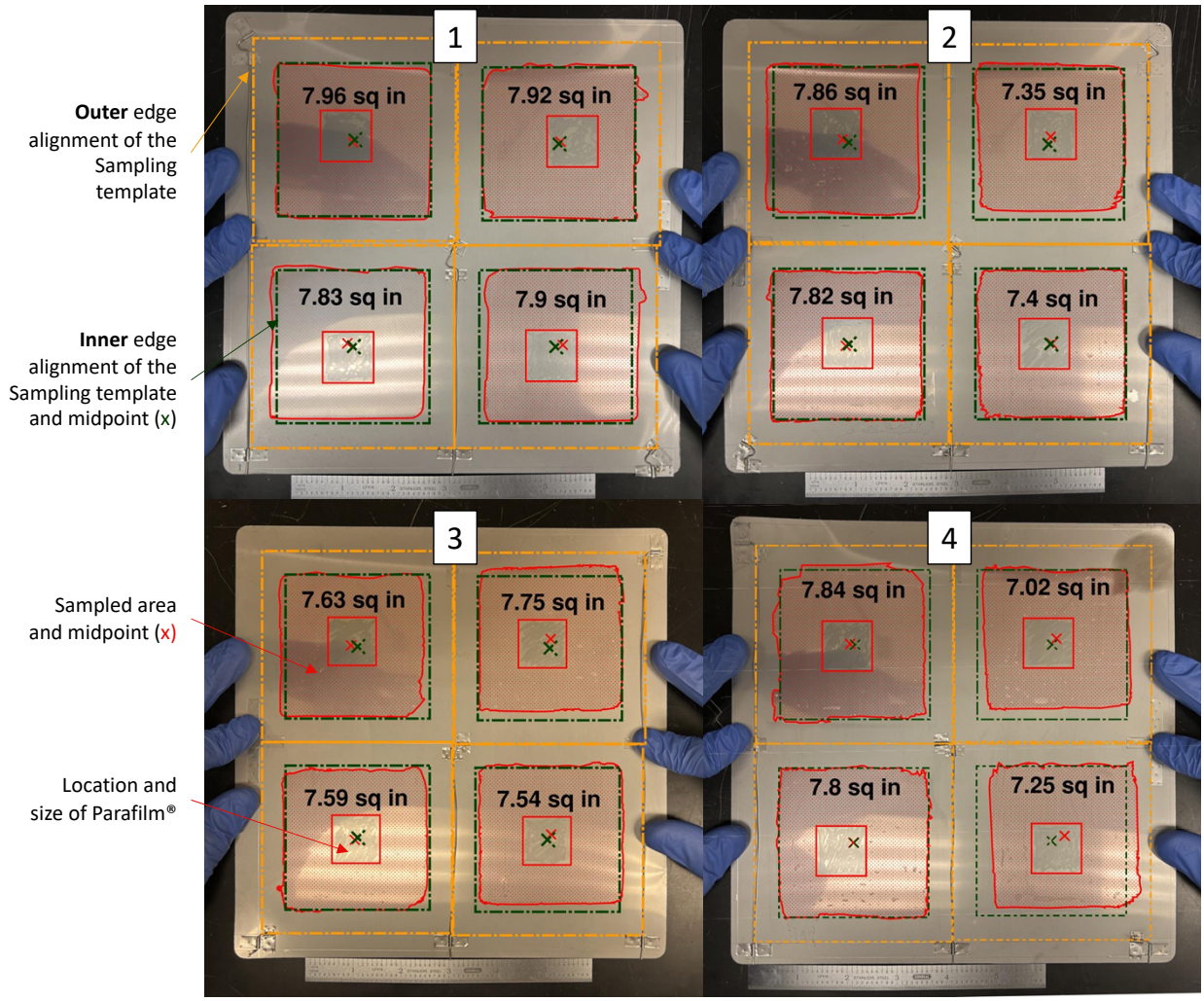

Figure 4.5 Picture of each of the sampled plates showing the proper alignment of the sampling template using the TC wires and shims. The outer edge of the tool is shown in orange and the sampling window is green. The actual area sampled is shown in red and the sampled areas are provided. The midpoints of the sampled area relative to the proper alignment are shown with the "x".

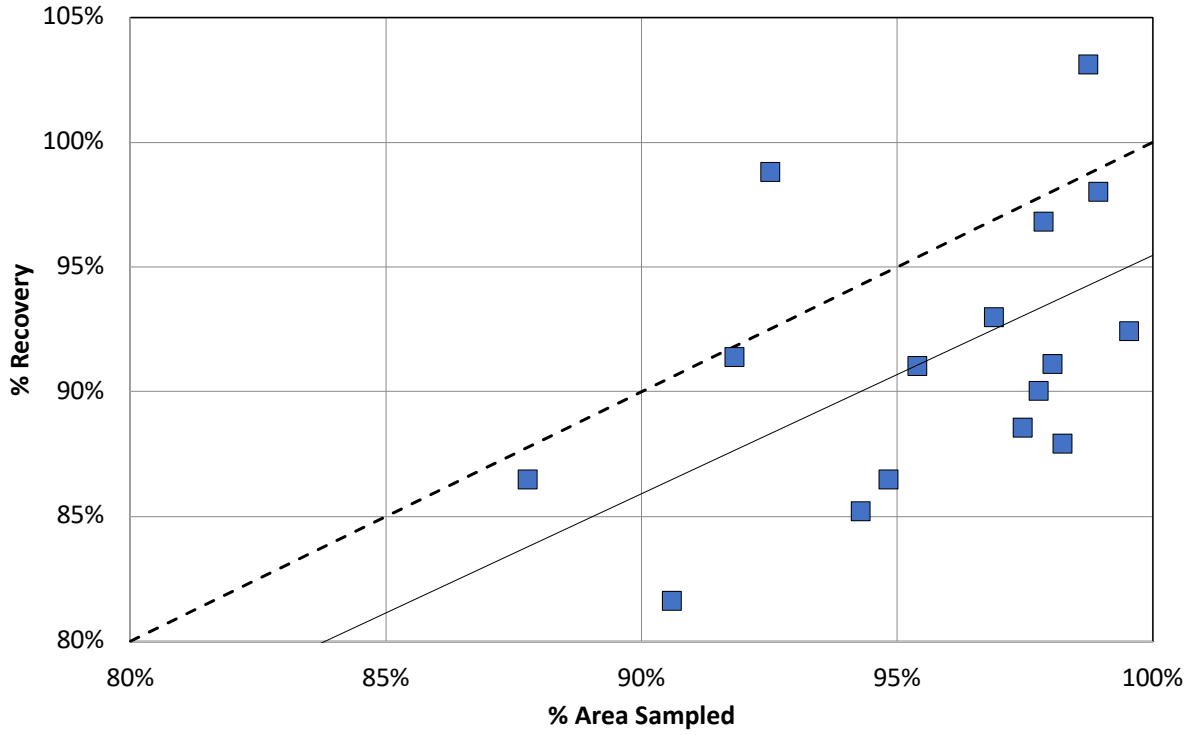

Figure 4.6 Percent salt recovery versus the percent area sampled shown with a 1:1 line.

The circumferential position on the canister appeared to impact the % salt recovery as well, as seen in Figure 4.7. During the dry run activity, it was anticipated that the top of the canister may have low recovery because the position felt very awkward. However this was not the case. The sampling efficiency was highest at the top of the canister (0º) and decreased moving circumferentially down the canister. The sampling efficiency of analyst 1 was relatively consistent from 40º to 120º, while the efficiency for analyst 2 decreased linearly with increasing circumferential position. However, another possible variable is the sampling order. The lowest sample, Plate 4 at 120º, was sampled first, and therefore it is possible that sampling improved with experience, as each analyst became more comfortable with the method and procedure.

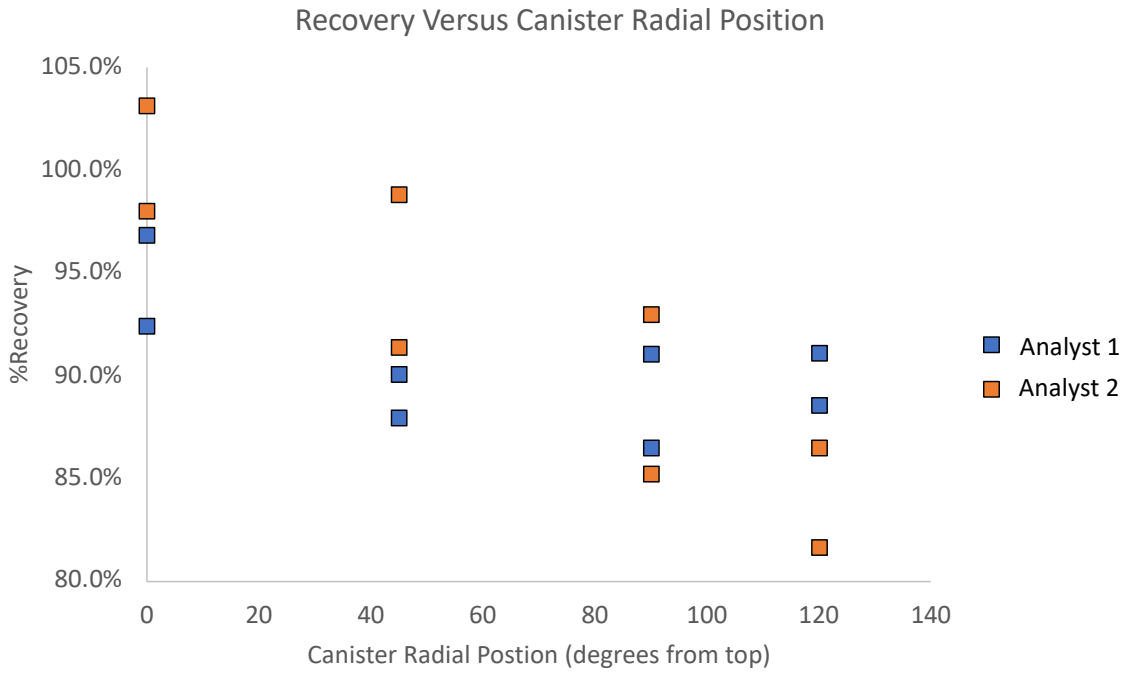

Figure 4.7 Percent salt recovery for each Analyst as a function of the canister radial position in degrees from the top of the canister (top = 0º)

Other factors that may impact the efficiency of salt recovery are the approximate sponge wetness and the salt loading on the metal surface. As previously documented, the wetness of the sponge appears to have a significant effect on salt recovery (Schaller *et al.*, 2022). In previous laboratory experiments, it was observed that the surface must be wet enough for the water to infiltrate the surface grooves and dissolve the salt. Sponge wetness was indirectly determined; the moistened sponges were not weighed directly, as including a weighing step for the actual sampling for the CDFD project would be very challenging. Instead, the sponges were weighed dry, and then total sample mass after adding water to leach the salts was determined. Since the mass of added water was known, the water in the sponge could be estimated by subtracting the dry sponge weight and the added water weight from the total sample weight. However, this is approximate, as a small amount of water remains on the surface after sampling, and that is not accounted for. The % salt recovery versus approximate sponge wetness is plotted in Figure 4.8a. There is considerable scatter, and no clear trend exists, although a weak trend was observed in the laboratory testing that had been done previously (Schaller *et al.*, 2022).

Another consideration was how salt loading impacts sampling efficiency. Figure 4.8b shows the % salt recovery versus the measured surface-area-normalized conductivity of the witness coupon (the assumed total salt loading). Similar to sponge wetness, there appears to be a trend, as the % salt recovery decreases as the conductivity, or salt loading, increases. Future experiments will further evaluate the impact of different salt loads on the sampling efficiency.

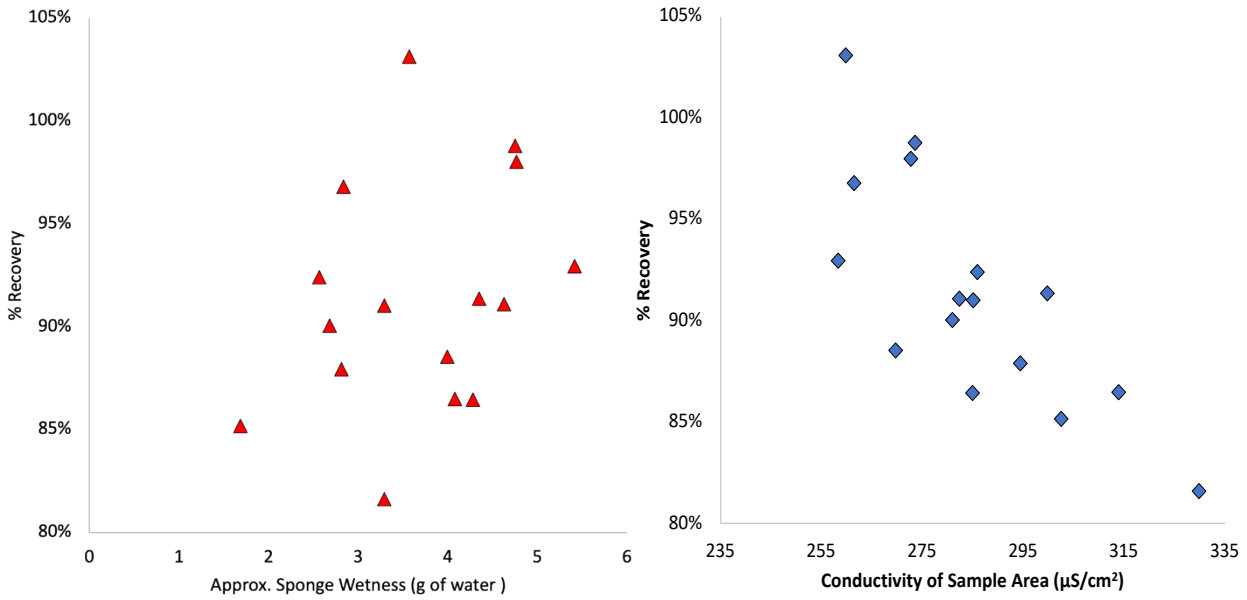

Figure 4.8 Percent salt recovery versus (a) approximate sponge wetness, and (b) total conductivity of the sample for each quadrant sampled.

4.2 Comparison to Controlled Laboratory Tests

The test described in this report, involving sampling from an actual canister mounted on a transfer skid mockup, is the first test to allow analysts to practice sampling methods in a prototypical environment with realistic access limitations. Previously, several tests had been performed in the laboratory on a 20 in. × 14 in. plate from mockup cylindrical canister shell built by SNL, which had approximately the same curvature and surface finish as a typical SNF dry storage canister (Enos and Bryan, 2016). The laboratory tests have been previously described (Knight *et al.*, 2022; Schaller *et al.*, 2022). Briefly, the plate was thoroughly cleaned and a sampling grid with 3 in. × 3 in. squares was spray-painted onto it using an engine enamel. Then, several SS witness coupons were attached to the surface with conductive carbon tape (to minimize static issues when coating the plate with salts) surrounding the sampling grid (Figure 4.9). The plate was coated with approximately 200-300 µg/cm^2 ASTM sea salts using a fogging chamber. This deposition method differed from the ink jet printer method used to coat the plates for this study, because the mockup canister plate used in the lab tests was too heavy for use in the ink jet printer. Following salt deposition, the witness coupons were removed from the plate surface and leached to extract the salts. The salt load on the witness coupons was used to map the salt distribution on the plate, and to estimate the salt load within the squares of the sampling grid. The sample plate had two sampling grids, and each analyst would sample one of the grids, with the sampling template and moist sponges, as described for the canister sampling. To quantify the salt present on the witness coupons and the sample areas, the surface-area-normalized conductivity of the leachates was measured as described in Section 4.

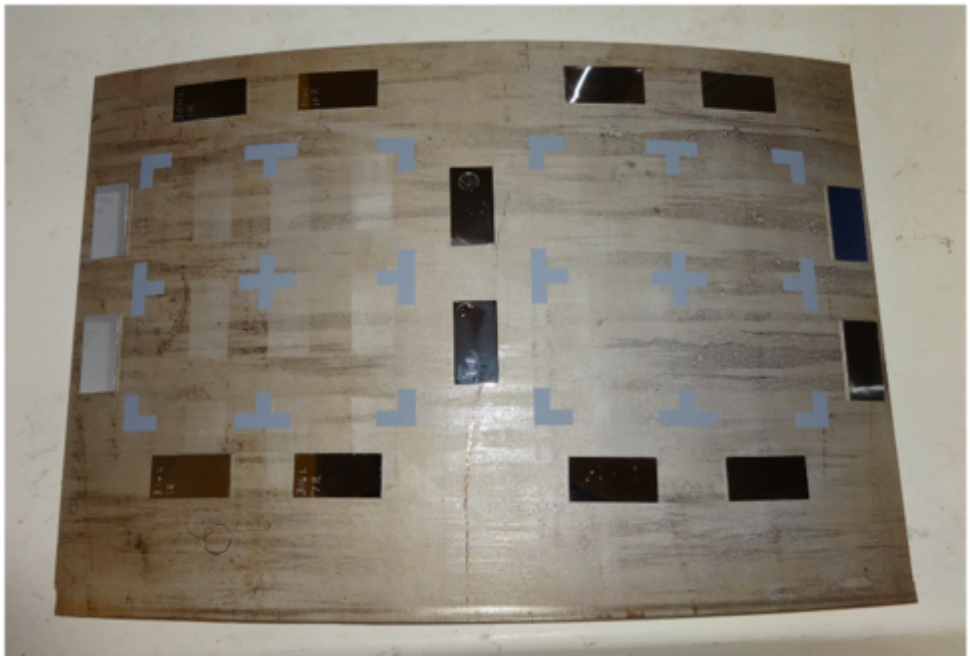

Figure 4.9 The SNL mockup canister plate, equipped with the sampling grid and witness coupons, used for the laboratory tests.

The average salt recovery for all 6 laboratory tests was 92 ± 6%. The results for the individual tests are provided in Table 4.2. In succeeding tests, methods were varied in an effort to increase the average % salt recovered and to decrease the variability; these generally had little effect; however, when attempts were made to deliberately vary the water content of the sponges, it was noted that drier sponges yielded somewhat less recovery. The results from the field test are consistent with the laboratory tests, averaging 91 ± 5 %.

Table 4.2 Average % recovery for both Analyst from laboratory tests 1-6.

Test	Average % Recovery
1	89 ± 6
2	85 ± 10*
3	97 ± 2
4	93 ± 5
5	89 ± 5
6	94 ± 4
Average from Laboratory Tests 1-6	92 ± 6

*Two outliers were removed. These outliers we not sufficiently equilibrated with the leaching solution, and the measured conductivity was far lower than expected for that reason.

The relationship between sponge wetness and the % salt recovery for all of the tests (Laboratory Test 1-6 and Outdoor Test 1) are shown in Figure 4.10. Throughout the experiments, the water content of the two sponges used for each sample cell varied from ~1 g to ~ 9 g. In general, sponges with less water resulted in less recovery of the salts, and recovery increased with sponge wetness, approaching 95% at water contents above 4-5 g. Notably, few tests were done with sponges containing >7 g of water as it was difficult to keep the sponge from dripping when removing it from the wetting solution. The data were fit to the following equation.

$$\%Salt\ Recovery = (1 - e^{(-k*sponge\ mass^n)}) \qquad \text{(Equation 2)}$$

The coefficients *k* and *n* were calculated using the MATLAB curve fitting module and were 1.43 and 0.48, respectively for Laboratory Tests 1-6. Overall, the equation reasonably captures the data trends; it is apparent that recovery increases slightly with increasing water content. When the data from Outdoor Test 1 are included in the fitting, the equation shifts slightly to k = 1.49 and n = 0.43.

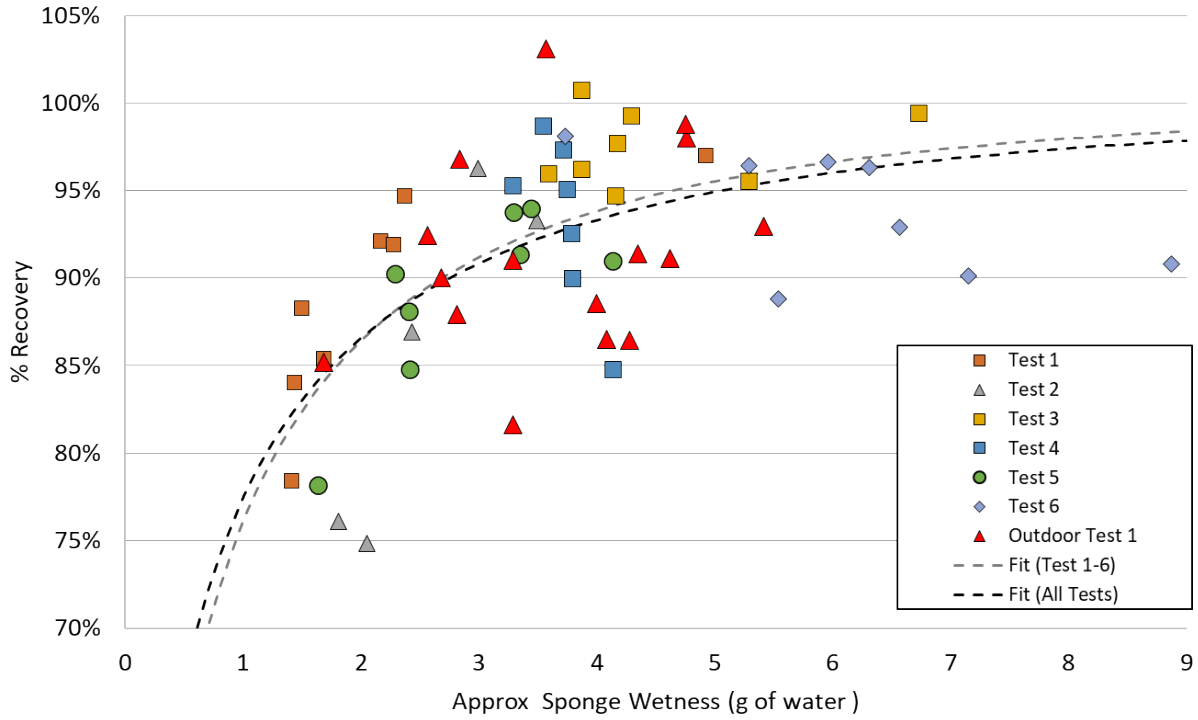

Figure 4.10 Percent salt recovery versus approximate sponge wetness for all tests.

The salt recovery versus the measured conductivity in shown in Figure 4.11 for Laboratory Tests 1-6 and Outdoor Test 1. This plot provides an understanding to how the salt load on the surface impacts the salt recovery. Overall, from Laboratory Tests 1-6, there appears to be a correlation between the salt load and the % salt recovered, as higher salt loadings had lower salt recoveries. Future work will more systematically evaluate how salt load impacts salt recovery. These relationships can help inform SNL on ways to improve the recovery when testing on the actual CDFD canisters and approximate the expected recovery based upon the sponge wetness or measured conductivity.

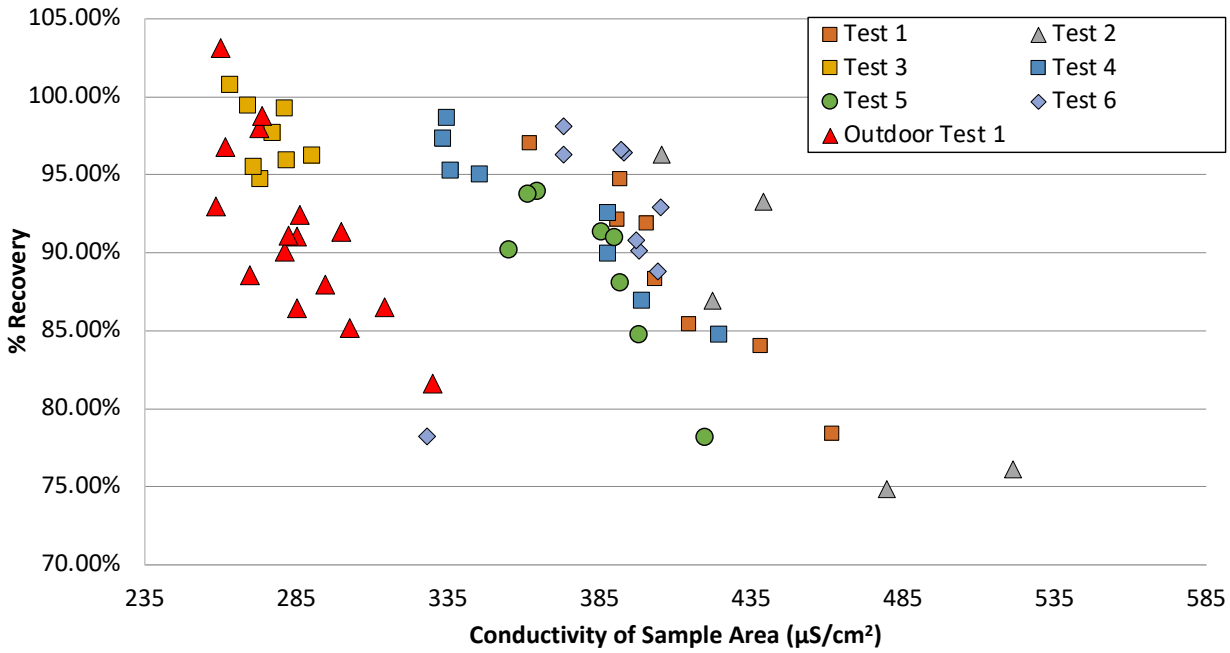

Figure 4.11 Percent salt recovery versus conductivity of the sampled region. This plot demonstrates the relationship between salt load and salt recovery.

This page is intentionally left blank.

5 DISCUSSION

Hand sampling the salts directly from the canister surfaces for the CDFD project provides a unique opportunity to develop and validate a high efficiency sampling strategy, providing reliable data for development and validation of a computational dust/salt deposition model. To date, SNL has analyzed salt and dust samples collected from 8 ISFSI sites. However, the sampling methods varied from site to site and the sampling efficiency of the methods is unknown, although in some cases, it is likely the surface is under sampled. The laboratory tests, and now the first outdoor test, have started to provide confidence in the sampling efficiency of the hand sampling method described in this report.

5.1 Analyst Variability

An important parameter to understand is variability in sampling efficiency associated with the identity of the analyst. To date, two analysts have performed 7 tests, both sampling a total of 23 different sample areas, in each case with essentially the same sampling method. A comparison of the salt recoveries for analysts 1 and 2 for all tests is shown in Figure 5.1. Overall, the results for the two analysts are consistent, where analyst 1 has an average recovery of 91 ± 5%, and analyst 2 averaged 92 ± 7 %. Figure 5.2 and Figure 5.3 summarize the performance of the two analysts in the 6 laboratory tests and in the outdoor test.

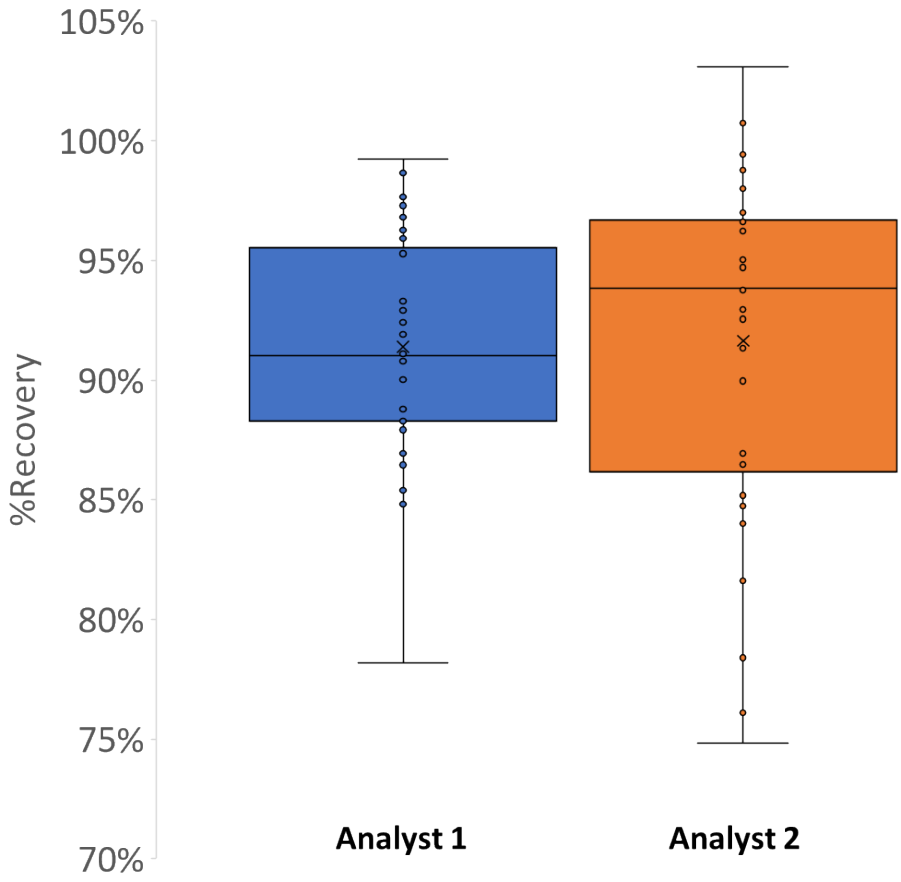

Figure 5.1 Box and whisker plot showing the sampling performance from all tests for analyst 1 and analyst 2.

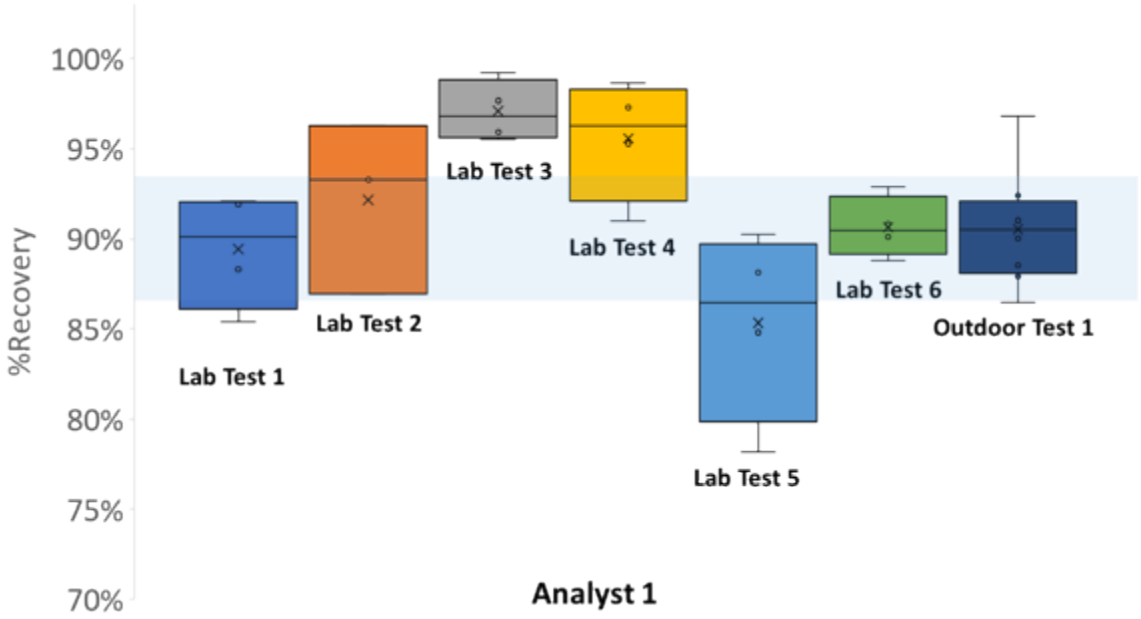

Figure 5.2 Box and whisker plot showing the sampling performance for each test for analyst 1.

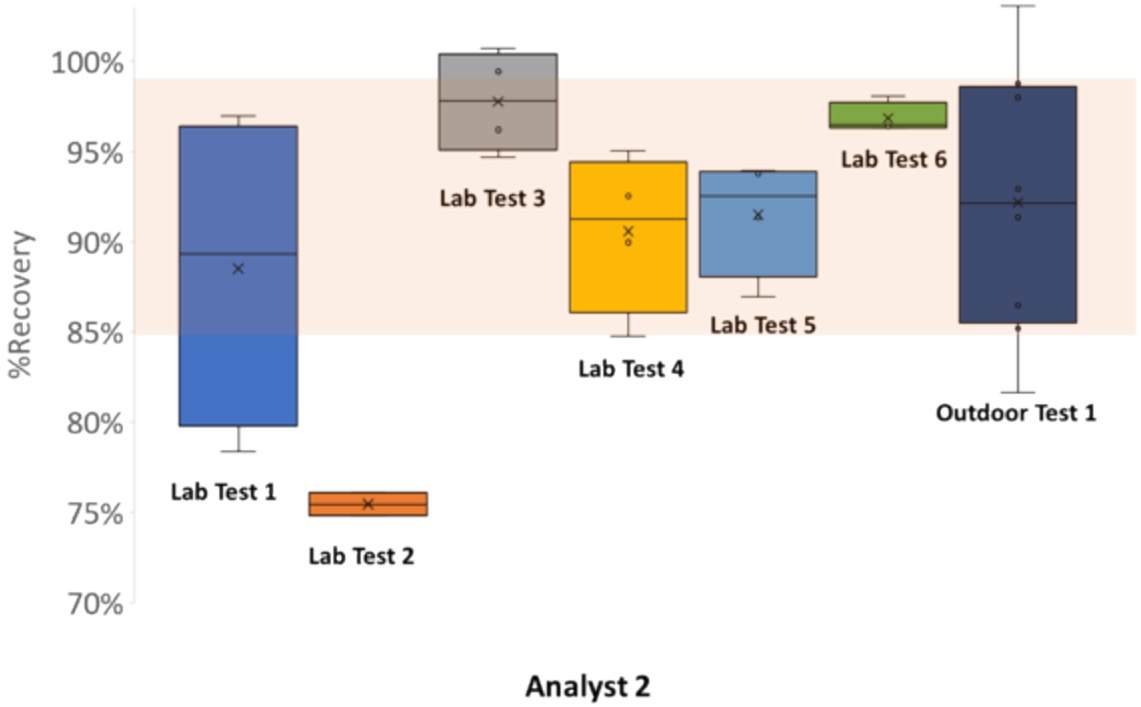

Figure 5.3 Box and whisker plot showing the sampling performance for each test for analyst 2.

An important factor for maintaining continuity over the entire lifetime of the CDFD project is an understanding of the analyst-to-analyst variability, and the potential impact of changes in the identity of the analysts over time. It will be important for each analyst to perform the exact same sampling procedure and to have practiced sufficiently to have a known and consistent sampling efficiency. If too much

variability is observed, effort must be made to identify and mitigate the inconsistencies in order to maintain analyst-to-analyst reliability. Any remaining variability must be insignificant relative to the measured dust/salt loads present on the canister during the CDFD test.

5.2 Lessons Learned

The field test described in this report, consisting of sampling the canister in place on top of the transfer skid mockup, was critical for developing and testing sampling procedures used by analysts on the boom lift. While this test successfully sampled the canister surface with efficiencies similar to those from previous laboratory tests, there were several lessons learned that will facilitate more effective sampling during the CDFD project.

- As discussed in Section 4.1.1, the sampling template alignment at some locations was not as prescribed by the sample shims. A few reasons for this include awkward approach angles and the lack of alignment features. While it may be difficult to improve surface access in some locations, ensuring that 4 shims define each square in a sample grid will likely aid in the alignment of the template.
- To facilitate sampling, both in terms of time and organization, a tray containing all the necessary sampling equipment should be designed and mounted to the boom lift carriage. Space is limited in the carriage and having a tray that extends off the end of the carriage would greatly aid sampling. The tray should have locations for several sample tubes, a DI reservoir to wet the sponges, a dry container to place the moist sponges, a holding tube for the tweezers, a holder for latex gloves, a rinsing station, garbage bags, and Kimwipes. This will not only decrease the sampling time, but also will also prevent cross contamination. The sampling tray is currently in the design stage, and it is anticipated that the tray will be incorporated prior to the next mockup test.
- For sampling on the actual CDFD canister, it will be important to have a mat that covers the floor of the boom lift carriage. This will prevent any unintended disruption of the canister surface during sampling, especially when sampling the top of the canister. In that position, the carriage is above the canister and anything falling from the lift (water, tools, or dirt) would fall onto the canister surface, potentially adding to or disrupting the dust on the surface.
- Finally, one possible way to improve the sampling efficiency would be to add a 3rd sponge to the sampling routine. This had not been done previously because the sample tubes could not accommodate 3 sponges. However, larger sample tubes have been acquired to test out this procedure. A 3rd sponge will be added to the sampling routine for the next canister mockup test to evaluate the impact.

5.3 Future Work

Prior to the first sampling campaign at the CDFD site, SNL will perform more sampling tests using the methods described in this report for the SNF canister mounted to the mockup transfer skid. The process will continue to be refined and understanding of the sampling efficiency will be developed. These developments will lead to a robust Standard Operating Procedure (SOP) for the actual sampling at the CDFD site.

The sample plates used the this first canister/skid test had a mirror polish, which does not reflect the expected canister surface roughness. For future tests, the sample plates will be roughened, likely by sandblasting, to a surface roughness that more closely resembles that of a real canister. The surface roughness of the canisters was measured indirectly via profilometry of a surface mold, as has been done previously (Knight et al., 2022; Schaller et al., 2022). The canister has a mill finish which previously been measured and equate to a roughness defined by $R_a = 0.79 \pm 0.04$ μm and $R_z = 4.19 \pm 0.3$ μm, which is equivalent to a 180-grit surface. The results from the first outdoor test did not vary significantly from the

previous laboratory tests on a mill-scale plate with a surface roughness similar to that of actual canisters, suggesting that surface roughness is not an important factor. However, it is best to keep the outdoor tests as realistic as possible.

Another variable that might be evaluated in future field tests is variable salt deposition. On actual canisters, it has been observed that the highest salt loads are generally present on the top and decrease as the surface becomes progressively steeper. For future outdoor tests, this observation can be mimicked by coating the plates with variable salt loads based on their circumferential location on the canister.

Based on field observations, dust loads on the top of the canister can be very heavy and consist largely in detrital mineral grains and organic materials, with only minor salts. The abundance of inert materials may make it difficult to quantitatively sample the dust and salts, although the sampling template has been designed with a trough for just such a condition. The sampling efficiency for heavy dust loads must be verified experimentally in future tests.

Lastly, for the future outdoor tests, a greater focus on timing will be evaluated. For operational reasons, it may be necessary to collect all samples on a given canister within a single workday. Hence, if sampling is too slow, the number of locations sampled in any given campaign may be impacted. Sampling two quadrants of a single sample grid (the number anticipated to be sampled during a real CDFD sampling campaign) in the first outdoor test took approximately 7-10 minutes, although it should be noted that only a single sample plate for each analyst was timed during the first outdoor test. This suggests that sampling a single complete column of 4 locations would take ~40 minutes. There are four complete columns, and one column with two sampling locations (Figure 3.11), which would take approximately 3 hours of sampling. With practice, this may be reduced with little or no loss of sampling efficiency. Fast, efficient sampling may be an important consideration when scheduling the sampling campaigns.

6 REFERENCES

Bryan, C., A. Knight, R. Schaller, S.G. Durbin, B. Nation, and P. Jensen, "Surface Sampling Techniques for the Canister Deposition Field Demonstration," SAND2021-3329 R, Sandia National Laboratories, Albuquerque, NM, March 2021.

Enos, D. and C. Bryan, "Final Report: Characterization of Canister Mockup Weld Residual Stresses," U.S. DOE. p. 62, 2016

Fascitelli, D.G., S. Durbin, and R.J.M. Pulido, "Status Update for the Canister Deposition Field Demonstration," SAND2022-8167 R, Sandia National Laboratories, Albuquerque, NM, June 2022.

Jensen, P.J., S. Suffield, C.L. Grant, C. Spitz, B. Hanson, S. Ross, S. Durbin, C. Bryan, and S. Saltzstein, "Preliminary Modeling of Chloride Deposition on Spent Nuclear Fuel Canisters in Dry Storage Relevant to Stress Corrosion Cracking," SAND2021-3570 J, Pacific Northwest National Laboratory, Richland, WA, 2021.

Knight, A., R. Schaller, B. Nation, S. Durbin, and C. Bryan, "FY22 Update: Development of Surface Sampling Techniques for the Canister Deposition Field Demonstration," SAND2022-4533 R, Sandia National Laboratories, Albuquerque, New Mexico, April 2022.

Lindgren, E.R., S.G. Durbin, S.R. Suffield, and J.A. Fort, "Preliminary Test Design and Plan for a Canister Deposition Field Demonstration," SAND2020-13075 R, Sandia National Laboratories, Albuquerque, NM, November 2020.

Schaller, R., A. Knight, R. Katona, B. Nation, E. Karasz, and C. Bryan, "FY22 Status Update: SNF Interim Storage Canister Corrosion and Surface Environment Investigations," SAND2023-10511 R, Sandia National Laboratories, Albuquerque, NM, September 2022.

Schindelholz, E. and R.G Kelly, "Application of Inkjet Printing for Depositing Salt Prior to Atmospheric Corrosion Testing," *Electrochemical and Solid State Letters*, 13(10): C29-C31, 2010.

Schindelholz, E., C. Bryan, and C. Alexander, "FY17 Status Report: Research on Stress Corrosion Cracking of SNF Interim Storage Canisters," SAND2017-10338R, Sandia National Laboratories, Albuquerque, NM, August 2017.

Suffield, S. R., Fort, J. A., Jensen, B. J., Perkins, W. A., Jensen, P. J., and C. Grant. "Update on Thermal and Deposition Modeling for the Canister Deposition Field Demonstration," M2SF-22PN0102080210, PNNL-31882, Pacific Northwest National Laboratory, Richland, WA, 2022.

Transnuclear Inc., Advanced NUHOMS System Updated Final Safety Analysis Report (UFSAR), Rev. 7, August 2016.

Transnuclear Inc., NUHOMS® HD System Safety Analysis Report (FSAR), Rev. 6, September 2017.

This page is intentionally left blank.


Sandia National Laboratories